

Efficient computation of linear response of chaotic attractors with one-dimensional unstable manifolds*

Nisha Chandramoorthy[†] and Qiqi Wang[‡]

Abstract. The sensitivity of time averages in a chaotic system to an infinitesimal parameter perturbation grows exponentially with the averaging time. However, long-term averages or ensemble statistics often vary differentiably with system parameters. Ruelle’s response theory gives a rigorous formula for these parametric derivatives of statistics or *linear response*. But, the direct evaluation of this formula is ill-conditioned and hence, linear response, and downstream applications of sensitivity analysis, such as optimization and uncertainty quantification, have been a computational challenge in chaotic dynamical systems. This paper presents the space-split sensitivity or the S3 algorithm to transform Ruelle’s formula into a well-conditioned ergodic-averaging computation. We prove a decomposition of Ruelle’s formula that is differentiable on the unstable manifold, which we assume to be one-dimensional. This decomposition of Ruelle’s formula ensures that one of the resulting terms, the stable contribution, can be computed using a regularized tangent equation, similar to in a non-chaotic system. The remaining term, known as the unstable contribution, is regularized and converted into an efficiently computable ergodic average. In this process, we develop new algorithms, which may be useful beyond linear response, to compute the unstable derivatives of the regularized tangent vector field and the unstable direction. We prove that the S3 algorithm, which combines these computational ingredients that enter the stable and unstable contributions, converges like a Monte Carlo approximation of Ruelle’s formula. The algorithm presented here is hence a first step toward full-fledged applications of sensitivity analysis in chaotic systems, wherever such applications have been limited due to lack of availability of long-term sensitivities.

Key words. Uniform hyperbolicity; Linear response; SRB measure; sensitivity analysis

1. Introduction. We say that a parameterized family of dynamical systems obeys *linear response* when the infinite-time averages or ergodic averages of its smooth observables vary differentiably with the parameter. It was shown by Ruelle [53][54] that uniformly hyperbolic maps, which are mathematical idealizations of chaotic attractors, follow linear response; Proposition 8.1 of [31] is a simplified proof using modern transfer operator techniques. Rigorous proofs of linear response have since been extended to uniformly hyperbolic flows [55], partially hyperbolic systems [26], dissipative stochastic systems [32], stochastically perturbed uniformly hyperbolic systems [40] and even to a larger class of stochastic systems with possibly non-hyperbolic unperturbed dynamics [29], certain nonuniformly hyperbolic systems [9] and intermittent systems [5][6][4]. From the statistical physics point of view, linear response theory has been found to be robust in high-dimensional systems [61][60], and has been usefully applied to chaotic systems across disciplines including climate models [52][51][10], biological systems (see [12] for a review of linear response in neuronal networks) and turbulent flows in

*Submitted to the editors DATE.

Funding: This work was funded by the Air Force Office of Scientific Research Grant No. FA8650-19-C-2207 and Department of Energy Research Grant No. DE-FOA-0002068-0018.

[†]Center for Computational Science and Engineering, Massachusetts Institute of Technology, Cambridge, MA (nishac@mit.edu).

[‡]Center for Computational Science and Engineering, Massachusetts Institute of Technology, Cambridge, MA (qiqi@mit.edu).

engineering systems [15][7][44][58].

Linear response of a chaotic system quantifies the proportional change in its long-term statistical behavior in response to small parameter perturbations. Apart from providing phenomenological understanding, this measure of long-term sensitivity is immensely useful in practical chaotic systems, which are often high-fidelity numerical simulations, for computational applications such as optimization, uncertainty quantification and parameter selection [24][7][8][15]. Particularly in climate science, theoretical as well as computational studies of violations of linear response and the presence of arbitrarily large linear responses [41][42][21][56] are crucial to gain a better understanding of intermittencies and climate tipping points [2], which are active areas of research.

Ruelle [53][54] established a formula for linear response or the derivative of ergodic averages with respect to parameters. However, a direct evaluation of this formula typically shows a poor convergence rate and is computationally impractical, as previous works have shown [14][28]. This poor convergence is due to the exponential growth of infinitesimal perturbations – the so-called butterfly effect – which is the defining characteristic of chaotic systems. Due to the butterfly effect, the sensitivity of a state at a time n into the future, to an infinitesimal perturbation to the current state in almost any direction, grows exponentially with n . Now, infinitesimal parameter perturbations may be thought of infinitesimal perturbations to each state applied in different tangent directions. Thus, along any trajectory, the sensitivity to an infinitesimal parameter perturbation also grows exponentially. However, the average of the sensitivities across all trajectories is a bounded quantity at all times. This ensemble-averaged sensitivity is, in fact, exponentially decreasing with time in uniformly hyperbolic systems, and Ruelle’s formula for linear response is a series summation of these ensemble-averaged sensitivities. But, ensemble averaging exponentially growing quantities is a computationally challenging task that shows poor convergence.

Traditionally, sensitivities in a dynamical system are estimated by using tangent or adjoint equation solutions, or through automatic differentiation. Since all these methods time-evolve infinitesimal perturbations about a reference trajectory, the sensitivities they compute grow exponentially along any trajectory. Hence, conventional methods for sensitivity analysis have long been recognized as unsuitable in chaotic systems for computing linear response. Some methods circumvent the problem of exponentially growing sensitivities to compute a bounded value for linear response, but they may exhibit a bias [36][48]. One such method is least-squares shadowing [59] and its non-intrusive version [48][47], in which the shadowing lemma (see e.g. Chapter 18 of [35]) is used to compute sensitivities along a shadowing orbit. However, since shadowing orbits may be nonphysical, i.e., ergodic averages along shadowing orbits may not converge to ensemble averages, the sensitivities computed by least-squares shadowing are not guaranteed to converge to linear response [19], although the error may be small for problems with a small ratio of unstable dimension to overall dimension [45].

Moreover, the direct evaluation of Ruelle’s formula may also be thought of as an adaptation of conventional tangent/adjoint-based sensitivity computations for chaotic systems. This direct evaluation, known as the ensemble sensitivity approach [37][28], involves taking a sample average of sensitivities computed by conventional tangent/adjoint methods. However, as we noted earlier, the number of samples needed, to reduce the variance in the exponentially growing sensitivities and compute linear response accurately, makes this approach computa-

tionally infeasible. In blended response algorithms [1], the ensemble sensitivity approach for short-time sensitivities is *blended* with a fluctuation-dissipation theorem-based approximation of the long-term sensitivities. This approximation is however adhoc since the densities of the SRB measure on unstable manifolds may not follow the fluctuation-dissipation theorem-based approximation, even though linear response holds.

The purpose of this paper is an efficient computation of linear response in chaotic dynamical systems. We remark that using transfer operator techniques, a rigorous computation of linear response has been developed before, but it has been restricted to low-dimensional expanding maps [3]. Our aim is to develop a numerical method to evaluate Ruelle’s formula that is scalable to high-dimensional practical systems. For this reason, we seek a method to compute Ruelle’s formula that is provably convergent and is a computable ergodic average, which does not involve discretization of the phase space. The latter property of trajectory-based computation ensures that the convergence is that of a Monte Carlo computation of Ruelle’s formula, at a rate independent of the system dimension.

In this paper, we develop the space-split sensitivity or the S3 method, which is a scalable, efficient and rigorous computation of linear response. We prove that S3 provably converges in uniformly hyperbolic systems, and the convergence rate is similar to a typical Monte Carlo integration. We focus on uniformly hyperbolic systems with one-dimensional unstable manifolds, but design S3 keeping in mind future extensions to systems that have an unstable manifold of arbitrary dimension.

2. Prior work on computation of Ruelle’s formula. Besides previous work referenced in the introduction (section 1), in this section we compare and contrast two recent methods on the computation of Ruelle’s formula against S3, which is developed in the present paper. In the computable realization of Ruelle’s formula that is developed in [16] (and expanded in [17]), we split the perturbation field into its components along unstable and stable subbundles. In uniformly hyperbolic systems, such a direct sum decomposition of a vector field into its components along unstable and stable subbundles exists, and the resulting stable and unstable vector fields are Hölder continuous on the phase space (Chapter 6, 19 of [35]).

In [16][17], a method is then developed to evaluate the two resulting terms of Ruelle’s formula. In the evaluation of the response to the unstable component, a finite difference is suggested to compute a part of the unstable divergence term [16][17]. Besides this cumbersome computation of the unstable divergence, the major limitation of the linear response computation in [16][17] is a fundamental differentiability assumption that generally does not hold in uniformly hyperbolic systems. In particular, in the computation of the unstable contribution, the unstable component of the perturbation field is differentiated in the unstable directions, and this derivative is computed partly by finite difference and partly by a recursive formula (section 5 of [17]). Underlying this differentiation of the unstable component is the implicit assumption that the stable component of the perturbation is also differentiable along the unstable directions (since the perturbation field, which is the sum of its stable and unstable components, is differentiable by assumption in all directions), and this differentiability does not hold in a generic uniformly hyperbolic system (even in the case of smooth dynamics [33, 50]).

By contrast, to derive S3, we prove a new decomposition of Ruelle’s formula – the S3

decomposition – which is differentiable on the unstable manifold. The S3 decomposition is not a stable-unstable splitting of the parameter perturbation vector field, which is pursued in [16][17]. In a slight abuse of terminology, the two resulting components of the S3 decomposition are still called the stable and unstable contributions to the overall sensitivity, although they do not arise from a stable-unstable splitting of the perturbation field. We develop recursive algorithms to compute the ingredients of both these components. The novel recursive algorithms for the stable and unstable contributions that are developed in this work do not use the covariant Lyapunov vector basis [11], unlike in [16][17]. We only require an orthonormal basis for the unstable subspace, which is computationally cheaper to obtain, and requires only forward iterations of the dynamics.

A recent work by Ni [46] introduces the linear response algorithm, which appears to be another viable solution to linear response computation. It has been derived for uniformly hyperbolic systems with arbitrary dimensional unstable manifolds. This algorithm provides a “fast” computation of the unstable divergence via a recursive formula, analogous to the density gradient for one-dimensional unstable manifolds treated in the present paper. In this linear response algorithm, second-order tangent equations, which are the most expensive step, are solved to differentiate certain vector fields with respect to a modified shadowing direction, which is computed by non-intrusive shadowing [48]. The second-order tangent equations developed in the present paper are derivatives along the one-dimensional unstable manifold.

The plan for the paper is as follows. In section 3, we introduce Ruelle’s linear response formula and provide the mathematical background for its decomposition and subsequent evaluation via the S3 algorithm. Section 4 is a concise statement of the main contributions of this paper: two theorems concerning the S3 decomposition and evaluation, and the S3 algorithm. In section 5, we derive the S3 decomposition of Ruelle’s formula. The computation of the stable contribution that results from the decomposition is discussed in 5.3. An alternative expression of the unstable contribution is derived in section 5.4, whose computation is tackled in section 6. The validation of S3 on perturbed Baker’s maps and Solenoid maps are presented in sections 7.1 and 7.2 respectively. The proofs of the two main theorems are split between sections 8 and 9. Section 8 proves the existence of the S3 decomposition and its differentiability in the unstable direction, while section 9 completes the proof of convergence of the S3 algorithm. In section 10, we summarize our contributions and present a roadmap for extending the present algorithm to systems with higher-dimensional unstable manifolds.

3. Preliminaries and problem setup. Consider a parameterized family $\varphi_s : M \rightarrow M$ of C^3 diffeomorphisms of a Riemannian manifold M , which we consider to be specified as a subset of \mathbb{R}^m . Let s be a scalar parameter that can take a small range of values around a reference value, say s_0 . Corresponding to infinitesimal parameter perturbations at s_0 , we define a vector field $\chi = d_s|_{s=s_0}\varphi_s \circ \varphi^{-1}$.

Suppose φ_s exhibits linear response at the reference value s_0 , which we associate with the unperturbed dynamics. This means that the parametric derivative of long-term averages of φ_s exists at the reference value s_0 . Thus, at any $s = s_0 + \delta s$ close to s_0 , up to first order in δs , the long-term averages of φ_s can be expressed using information associated only to the dynamics φ_{s_0} . Let $J \in C^2(M)$ be an observable of interest, e.g. a lift or a drag in a numerical simulation of a turbulent flow. We are interested in a quantitative determination of how the

long-term average of J responds to infinitesimal perturbations in s , at s_0 , i.e., to perturbations in the direction χ .

3.1. Ergodic theory and linear response. The infinite-time average of J is defined as $\langle J \rangle(x) := \lim_{N \rightarrow \infty} (1/N) \sum_{n=0}^{N-1} (J \circ \varphi_s^n)(x, s)$, for $x \in M$. A probability distribution over the states on M , μ_s is stationary or φ_s -invariant, when $\mu_s(\varphi_s^{-1}A) = \mu_s(A)$, for any Borel subset $A \subseteq M$. When μ_s is an ergodic, φ_s -invariant, physical probability distribution for φ_s , infinite-time averages, also known as ergodic averages, are equal to expectations with respect to μ_s , at Lebesgue almost every x in the basin of attraction of φ_s . The expectation or ensemble average of an observable J with respect to μ_s , which is the Lebesgue integral with respect to the distribution μ_s , is written as $\langle J, \mu_s \rangle$.

That is, in ergodic systems, $\langle J \rangle(x, s)$ is independent of x – it is only a function of s – and equal to $\langle J, \mu_s \rangle$ at almost every x in a set of full Lebesgue measure. The quantity we wish to compute is *linear response* at s_0 , which is the parametric derivative of the ergodic/ensemble average, $d_s|_{s_0} \langle J, \mu_s \rangle$. When J explicitly depends on s and the dependence is smooth, $d_s \langle J, \mu_s \rangle = \langle J, \partial_s \mu_s \rangle + \langle \partial_s J, \mu_s \rangle$. The second term, $\langle \partial_s J, \mu_s \rangle$ is simply an ergodic/ensemble average of $\partial_s J$, which can be computed, using its definition, along almost every orbit:

$$\langle \partial_s|_{s_0} J, \mu_{s_0} \rangle = \lim_{N \rightarrow \infty} (1/N) \sum_{n=0}^{N-1} (\partial_s J)(\varphi_{s_0}^n x, s_0),$$

for Lebesgue almost every x on M . Since this does not pose a computational challenge, we neglect the explicit dependence of J on s , and focus on the first term, $d_s|_{s_0} \langle J, \mu_s \rangle = \langle J, \partial_s|_{s_0} \mu_s \rangle$. From here on, we denote linear response at s_0 simply as $\langle J, \partial_s \mu_s \rangle$, for brevity.

3.2. Tangent dynamics. The tangent space at $x \in M$, denoted $T_x M$, is the space of all infinitesimal perturbations to x , which can be identified with \mathbb{R}^m . A vector field on M , which is a direction of infinitesimal perturbation to the state at each point on M , can be considered as a map from M to \mathbb{R}^m . If v is a vector field and $x \in M$, then $v_x \in T_x M \equiv \mathbb{R}^m$ denotes the value of the vector field at x . Fixing s at its reference value, we denote φ the map φ_{s_0} . Similarly, we refer to the distribution μ_{s_0} simply as μ .

The matrix $d\varphi^n$ gives the pushforward of a vector field by φ^n . That is, $w = d\varphi^n v$ if $w_{\varphi^n x} = d\varphi_x^n v_x$. We write $d\varphi^1$ simply as $d\varphi$. In the context of computations, we often fix a particular reference trajectory, say $\{x_n\}$, where x_0 is sampled according to μ . We denote values of a vector field v along the reference trajectory using $v_n := v_{x_n}$ for short; similarly, we write $(d\varphi)_n$ to denote the value of $d\varphi$ at x_n . The homogeneous tangent equation tracks the pushforward by φ^n along a fixed trajectory,

$$(3.1) \quad u_{n+1} = (d\varphi)_n u_n, \quad n \in \mathbb{Z}^+.$$

At every iteration of the homogeneous tangent equation, starting with $u_0 \neq 0 \in \mathbb{R}^m$, the vector field u is updated to $d\varphi u$. When we add a source term to Eq. 3.1, we refer to the resulting equation as the inhomogeneous tangent equation. For example, when the source term is the parameter perturbation field, $\chi := (\partial_s \varphi_s)(\varphi_{s_0}^{-1} \cdot, s_0)$, the inhomogeneous tangent equation is the conventional tangent equation that is standard in sensitivity analysis,

$$(3.2) \quad u_{n+1} = (d\varphi)_n u_n + \chi_{n+1}.$$

In this tangent equation, at every iteration, the vector field u is updated to $d\varphi u + \chi$. In tangent sensitivity analysis, the parametric derivative of time-averages, $\partial_s(1/N) \sum_{n=0}^{N-1} (J \circ \varphi_s^n)(x_0, s_0)$, is usually computed using inhomogeneous tangent solutions (Eq. 3.2) as

$$\frac{1}{N} \sum_{n=0}^{N-1} \partial_s(J \circ \varphi_s^n)(x_0, s_0) = \frac{1}{N} \sum_{n=0}^{N-1} dJ(x_n) \cdot u_n.$$

Everywhere, d denotes the gradient operator in \mathbb{R}^m . For example, in the above equation, $dJ(x_n) = (dJ)_n \in \mathbb{T}_{x_n}^* M \equiv \mathbb{R}^m$ refers to the gradient of J evaluated at the point x_n .

3.3. Chaotic systems. The Oseledets multiplicative ergodic theorem (OMET) says that the homogeneous tangent solutions (Eq. 3.1) grow/decay asymptotically. Further, this asymptotic growth/decay is exponential at a finite number of rates, called the Lyapunov exponents, which, in our setting of ergodic systems, are independent of the starting point x_0 , at μ_s almost every x_0 . We denote them in descending order as $\lambda_1 > \lambda_2 > \dots > \lambda_p$, with $p \leq d$. A chaotic system, by definition, exhibits at least one positive Lyapunov exponent.

The tangent space at μ -almost every point $x \in M$ has a direct sum decomposition, $T_x M = \bigoplus_{i \leq p} E_x^i$, with the subspace E_x^i of tangent vectors having the asymptotic growth/decay rate λ_i . In other words, every tangent vector v_x belonging to the subspace E_x^i is such that $\lim_{n \rightarrow \infty} (1/n) \log \|d\varphi_x^n v_x\| = \lambda_i$. At μ -almost every x_0 , almost every choice of $u_0 \in \mathbb{R}^m$ will have a non-zero component on the tangent subspace corresponding to the largest positive Lyapunov exponent. Hence, in chaotic systems, homogeneous tangent solutions starting from every initial condition u_0 grow exponentially in time. That is, for almost every $u_0 = u(x_0)$, $\|u_n\| \sim \mathcal{O}(e^{\lambda_1 n})$, with $\lambda_1 > 0$, for large n . The exponent λ_1 , which determines the asymptotic growth factor of the tangent solutions, is the largest among the Lyapunov exponents.

3.4. Uniform hyperbolicity. In this paper, we consider our C^3 diffeomorphism $\varphi : M \rightarrow M$ to be equipped with a compact, invariant, hyperbolic attractor Λ , which contains a one-dimensional unstable manifold. That is, Λ is a compact set and $\varphi(\Lambda) = \Lambda$. We say Λ is a hyperbolic set for φ if there exist constants $C > 0$ and $\lambda \in (0, 1)$ such that, at every point $x \in M$, the tangent space $T_x M$ has a direct sum decomposition $T_x M = E_x^u \oplus E_x^s$, where

- E_x^u and E_x^s are φ -invariant, or *covariant*, subspaces. That is, $d\varphi_x(E_x^u) = E_{\varphi(x)}^u$ and $d\varphi_x(E_x^s) = E_{\varphi(x)}^s$.
- E_x^u is the 1-dimensional *unstable* subspace consisting of all $v \in T_x M$ such that

$$(3.3) \quad \|d\varphi_x^n v\| \leq C \lambda^n \|v\|,$$

for all $n \in \mathbb{Z}^-$, and,

- E_x^s is the $(m-1)$ -dimensional *stable* subspace consisting of all $v \in T_x M$ such that

$$(3.4) \quad \|d\varphi_x^n v\| \leq C \lambda^n \|v\|$$

for all $n \in \mathbb{Z}^+$.

Throughout, we use the shorthand $d\varphi_x$ to write the differential of φ at x , which is a linear map from $T_x M$, the tangent space at x , to $T_{\varphi x} M$, the tangent space at φx . Using the standard basis of \mathbb{R}^m , $d\varphi_x$ can be represented as an $m \times m$ matrix.

Notation 3.1. For convenience, we write f_x to denote a scalar, vector or tensor field f evaluated at the point $x \in M$.

3.5. The SRB measure. An ergodic, φ_s -invariant, physical measure, also known as an SRB measure [63], is guaranteed to exist in our setting of uniformly hyperbolic systems. Apart from φ_s -invariance, we use the ergodicity of the map φ_s with respect to μ_s , which implies that there is no subset of the attractor, other than itself, that is invariant under the dynamics and has full μ_s measure. We also employ the physicality of the SRB measure. This means that ergodic averages starting from Lebesgue-a.e. initial condition chosen in an open set containing the attractor converge to expected values with respect to μ_s .

We also exploit exponential decay of correlations with respect to the SRB measure enjoyed by observables in uniformly hyperbolic systems [22][39][62]. This means that, for two Hölder continuous observables J and f , there is some $c > 0$ and $\delta \in (0, 1)$ so that $|\langle J \circ \varphi^n f \rangle - \langle J \rangle \langle f \rangle| \leq c \delta^n$, for all $n \in \mathbb{Z}^+$. In the S3 algorithm, we often deal with Hölder continuous functions that have zero expectation, in which case, we use $|\langle J \circ \varphi^n f \rangle| \leq c \delta^n$. As a result of exponential decorrelation, Hölder observables also satisfy the central limit theorem (CLT) and the law of the iterated logarithm which implies that for almost every $x \in M$, the error in the N -time ergodic average of a Hölder observable J declines asymptotically as $\mathcal{O}(\sqrt{\log \log N} / \sqrt{N})$: $|(1/N) \sum_{n=0}^{N-1} J_{\varphi^n x} - \langle J \rangle| \leq c \sqrt{\log \log N} / \sqrt{N}$, for large N and some $c > 0$.

Further, we use the fact that the SRB measure, although typically singular with respect to Lebesgue measure on \mathbb{R}^m , has absolutely continuous conditional measures on the unstable manifold. We shall next elaborate on this property as used in the derivation of the S3 algorithm (section 4.1).

3.6. Parameterization of unstable manifolds. The unstable subspace is tangent to the local unstable manifolds. Given an $\epsilon > 0$, a local unstable manifold at an $x \in \Lambda$, $U_{x,\epsilon}$, contains points whose backward orbits lie ϵ -close to the backward orbit of x . That is,

$$U_{x,\epsilon} = \left\{ x' \in M : \|x_{-n} - x'_{-n}\| \leq \epsilon, \forall n \in \mathbb{Z}^+; \lim_{n \rightarrow \infty} \|x_{-n} - x'_{-n}\| = 0 \right\}.$$

Since E_x^u are one-dimensional subspaces, the local unstable manifolds are also one-dimensional. According to the stable-unstable manifold theorem (see e.g. Theorem 6.2.8 of [35], [27]), the local unstable manifolds are embedded images of Euclidean spaces of the same dimension, which in this case are real lines.

In this paper, we work with a particular C^1 parameterization of local unstable manifolds. Let Ξ be a measurable partition of Λ that is subordinate to the unstable manifold, and let Ξ_x denote the element of the partition containing x . At each x , we can choose an ϵ depending on x so that Ξ_x contains a local unstable manifold at every x . We choose a parameterization $\Phi^x : [-\epsilon_x, \epsilon_x] \rightarrow \Xi_x$ that satisfies the following properties:

1. $\Phi^x(0) = x$
2. $d_\xi \Phi^x(\xi) = q_{x'}$, where $\Phi^x(\xi) = x'$, for all x' in the image of Φ^x .

Such a measurable function $x \rightarrow \epsilon_x$ exists that allows the definition of Φ^x (see Chapter 6 of [35]; [38]). Here $q_{x'} \in T_{x'}M$ is the unit vector in the one-dimensional tangent subspace $E_{x'}^u$. From 2., it follows that $\|d_\xi \Phi^x((\Phi^x)^{-1}(x'))\| = 1$, for all x' in the image of Φ^x . Hence we refer to the pointwise coordinate maps Φ^x as the unit speed parameterization of local unstable manifolds.

3.7. Iterative differentiation on the unstable manifold. The orbits of φ^{-1} starting in Ξ_x generate corresponding orbits on the real line by this parameterization. More concretely, we define the dynamics on the real line, through the map $(\tilde{\varphi}^x)^{-1} := \left(\Phi^{(\varphi^{-1}x)}\right)^{-1} \circ \varphi^{-1} \circ \Phi^x$. We frequently use the following relationship that can be derived using the chain rule, where d_ξ denotes differentiation with respect to the coordinate ξ :

$$(3.5) \quad d_\xi (\tilde{\varphi}^x)^{-1}(\xi) = \frac{1}{\alpha_{x'}},$$

Here $\Phi^x(\xi) = x'$, and α is the scalar field that represents the local expansion factor.

Definition 3.2. We define a scalar field $\alpha : M \rightarrow \mathbb{R}^+$ to capture the local expansion of unstable tangent vectors. At each $x \in M$,

$$(3.6) \quad \alpha_x = \|d\varphi_{\varphi^{-1}x} \varphi_{\varphi^{-1}x}\|.$$

Notice that the derivative of $(\tilde{\varphi}^x)^{-1}$ with respect to the unstable coordinate ξ does not depend on the base point of the coordinate system, x . This fact is crucial to the derivation of the S3 algorithm, where we prominently differentiate scalar and vector fields “on unstable manifolds” of a reference orbit. We now describe what this differentiation means in this paper, and a formula useful for performing this differentiation recursively.

Let $x_0 \in M$ be a fixed μ -typical point whose forward orbit serves as the reference orbit for our computation. Let $f : M \rightarrow \mathbb{R}$ be a scalar field, and h be the scalar field that represents the derivative of f on the unstable manifold. We define this function, using our coordinate systems centered on $\{x_n\}$ as follows, $h_{x'_n} := d_\xi(f \circ \Phi^{x_n})(\Phi^{x_n})^{-1}(x'_n)$, for some $x'_n \in \Xi_{x_n}$.

Now suppose we wish to compute h recursively along an orbit; the situation where such a computation arises in the S3 algorithm is discussed in section 6. To compute the values h_{x_n} using $\{h_{x_m}\}_{m < n}$, we use the following iteration that in turn uses Eq. 3.5,

$$(3.7) \quad \begin{aligned} d_\xi(f \circ \varphi \circ \Phi^x)(0) &= d_\xi(f \circ \Phi^{\varphi x} \circ \tilde{\varphi}^{\varphi x})(0) \\ &= h_{\varphi x} \alpha_{\varphi x}. \end{aligned}$$

We sometimes use the notation $\partial_\xi f$ to denote h , which we simply refer to as the unstable derivative of f .

3.8. Conditional density of the SRB measure on unstable manifolds. An important property of the SRB measure, which guarantees its physicality, is its absolute continuity along unstable manifolds [63]. To define this property, we must introduce conditional densities of the SRB measure on the unstable manifold, which we denote ρ . We may define the function ρ using our parameterization $\{\Phi^x\}$ and disintegration to yield a family of functions $\{\rho^x\}$. It is worth noting that changes to the parameterization only affect the normalization constant of the densities ρ^x . By the disintegration of SRB measure [38][23] on the measurable partition Ξ , there exist i) a family of conditional measures denoted μ^x , at μ -a.e. $x \in M$, that are supported on Ξ_x , and ii) a quotient measure $\hat{\mu}$ on M/Ξ , such that, for all Borel subsets $A \subseteq M$,

$$(3.8) \quad \mu(A) = \int_{M/\Xi} \mu^x(A \cap \Xi_x) d\hat{\mu}(x).$$

An aside on the notation used henceforth: a phase point $x \in M$ that appears in the superscript indicates the point at which our pointwise coordinate system is centered; this is distinct from its appearance on a subscript, which always means evaluation of a scalar/vector field at x . Let ν^x be the normalized pushforward of the Lebesgue measure (uniform probability distribution) on $[0, 1]$, by Φ^x . The absolute continuity property of the SRB measure on the unstable manifold means that the conditional measure μ^x is absolutely continuous with respect to ν^x . Thus, a scalar function ρ^x can be defined as the *probability density* of μ^x . In particular, the unnormalized density ρ_u^x of μ^x has been derived by Pesin [49][34] to be,

$$(3.9) \quad \rho_u^x(x') := \prod_{k=0}^{\infty} \frac{\alpha_{\varphi^{-k}x}}{\alpha_{\varphi^{-k}x'}},$$

where the local expansion factor α is as defined in Eq. 3.6.

Definition 3.3. *The probability density of conditional SRB measures on the unstable manifold is defined as $\rho^x(x') = \rho_u^x(x')/\bar{\rho}^x$, for $x' \in \Xi_x$, where $\bar{\rho}^x := \int_{\Xi_x} \rho_u^x(x') d\nu^x(x')$, is the normalization constant.*

Using the above definition of the density, the disintegration of the SRB measure on the unstable manifold (Eq. 3.8) gives, for any smooth observable f ,

$$(3.10) \quad \langle f \rangle = \int_{M/\Xi} \int_{\Xi_x} f(x') \rho(x') d\nu^x(x') d\hat{\mu}(x).$$

3.9. Linear response of uniformly hyperbolic systems. Ruelle [53][54] showed that linear response holds and is given by the following formula in uniformly hyperbolic attractors,

$$(3.11) \quad \langle J, \partial_s \mu_s \rangle = \sum_{k=0}^{\infty} \langle d(J \circ \varphi^k) \cdot \chi, \mu \rangle,$$

where, as usual, we have dropped the subscript on φ and μ to indicate their respective values at $s = s_0$. According to Ruelle's formula (3.11), linear response or the parametric derivative of statistics, is a series summation of ensemble averages. The sensitivity of the function $J \circ \varphi^k$ to the parameter perturbation χ is given by $d(J \circ \varphi^k) \cdot \chi$, and the k th term in Ruelle's formula is an ensemble average of this instantaneous sensitivity. With probability 1, the instantaneous sensitivity, $d(J \circ \varphi^k) \cdot \chi$, grows in norm exponentially with k since χ almost surely has a non-zero component in E^u . But, due to cancellations over phase space, the ensemble average is bounded at all k . Further, the convergence of Ruelle's series implies that the ensemble average of instantaneous sensitivities decreases asymptotically with time and converges to zero.

Numerically, the direct evaluation of Ruelle's formula (3.11) involves approximating each ensemble average (each term in the series) as a sample average of instantaneous sensitivities. These instantaneous sensitivities are, in turn, computed by using the conventional tangent equation (section 3.2) or when the dimension of the parameter space is large, using the adjoint equation [48][28][14]. One may also use automatic differentiation in the forward and reverse mode to approximate the tangent and adjoint solutions respectively. However, the resulting sensitivity from any linear perturbation method increases exponentially with k at the rate of

the largest Lyapunov exponent, λ_1 ; hence considering the sample average of the sensitivities as a random variable, its variance increases as $\mathcal{O}(e^{2\lambda_1 k})$. Thus, the number of samples needed to approximate the integral accurately rapidly increases with k . On the other hand, thresholding the series computation (Eq. 3.11) at a small value of k to reduce the variance introduces a bias. This bias-variance trade-off has been analyzed in previous works [28][14], and the direct evaluation of Ruelle's formula rendered infeasible in practical systems.

4. Main results: S3 decomposition and computation of Ruelle's response formula.

The two key ideas that enable an efficient computation of Ruelle's formula are i) a particular decomposition of the perturbation field χ that splits Ruelle's formula into *stable* and *unstable* contributions, and ii) the development of iterative, ergodic-averaging evaluations of these two components. The first main result concerns the specific decomposition of a given parameter perturbation that we show enables an efficient computation.

Theorem 4.1. *A differentiable vector field χ has a sequence of decompositions $\chi = a^n q + (\chi - a^n q)$, where q is the unit vector field tangent to the one-dimensional unstable manifold, such that*

1. *the sequence of vector fields, $\{v^n\}_{n \in \mathbb{Z}^+}$ that satisfies*

$$(4.1) \quad v^{n+1} := d\varphi v^n + (\chi - a^{n+1}q), \quad n \in \mathbb{Z}^+,$$

with v^0 being any bounded vector field that is differentiable on the unstable manifold, converges uniformly; the sequence of scalar fields $\{a^n\}$ is chosen to orthogonalize v^n to the unstable manifold: $v_x^n \cdot q_x = 0$, at all $x \in M$ and for all $n \in \mathbb{Z}^+$;

2. *the sequence $\{a^n\}$ is differentiable on the unstable manifold and uniformly converging; and,*
3. *the sequence of unstable derivatives of $\{a^n\}$, namely, $\{b^n := \partial_\xi a^n\}$ converges uniformly.*

Let the limits of the sequences we introduced in Theorem 4.1 be denoted as follows: $a := \lim_{n \rightarrow \infty} a^n$, $v := \lim_{n \rightarrow \infty} v^n$ and $b := \lim_{n \rightarrow \infty} b^n$. From Theorem 4.1-2. and 4.1-3., the scalar field b is the unstable derivative of a , i.e., $b = \partial_\xi a$. We use the sequence $\{v^n\}$ to split Ruelle's formula into two computable infinite series. Fixing some finite K that controls the accuracy of the implementation, the S3 decomposition can be construed as a sequence of decompositions of χ into $\chi = (a^{K-k} q) + (\chi - a^{K-k} q)$, $0 \leq k < K$, wherein the former component is tangent to the unstable manifold. This gives the following decomposition, which converges to Ruelle's formula, as $K \rightarrow \infty$,

$$(4.2) \quad \langle J, \partial_s \mu_s \rangle = \lim_{K \rightarrow \infty} \sum_{k=0}^{K-1} \langle d(J \circ \varphi^k) \cdot (\chi - a^{K-k} q), \mu \rangle + \lim_{K \rightarrow \infty} \sum_{k=0}^{K-1} \langle d(J \circ \varphi^k) \cdot a^{K-k} q, \mu \rangle.$$

We refer to the first term on the right hand side as the *stable contribution*, and the second as the *unstable contribution* to the overall sensitivity. In section 5, we use Theorem 4.1 to show that the stable and unstable contributions can be alternatively expressed in the following

forms that are amenable to their computation.

$$(4.3) \quad \langle J, \partial_s \mu_s \rangle = \langle dJ \cdot v, \mu \rangle - \lim_{K \rightarrow \infty} \sum_{k=0}^{K-1} \langle J \circ \varphi^k (a^{K-k} g + b^{K-k}), \mu \rangle,$$

where we have introduced the *logarithmic density gradient* g , which is defined, for $x \in \Xi_{x'}$, as

$$(4.4) \quad g_x := \frac{1}{\rho^{x'}(x)} \frac{d(\rho^{x'} \circ \Phi^{x'})}{d\xi} ((\Phi^{x'})^{-1}(x)).$$

The intuition for the S3 decomposition is developed in section 5, and the proof of Theorem 4.1 is presented in section 8.

4.1. The S3 algorithm. The S3 algorithm is an efficient computation of the above split Ruelle's formula (Eq. 4.3). The computation of the different ingredients of this new formula as an efficient ergodic average is the other major contribution of this paper. In particular, we develop iterative algorithms to compute v , g and b along trajectories. Before we detail the S3 algorithm, we recall an important notation used throughout this paper.

Notation 4.2. When a μ -typical phase point $x_0 \in M$ is fixed, the subscript n applied to a scalar function or a vector field, denoted f , refers to its corresponding value at x_n . That is, when $x_0 \in M$ is fixed, $f_n := f_{\varphi^n x_0} = f_{x_n}$.

The S3 algorithm is as follows:

1. Obtain a long primal trajectory $x_{-K'}, \dots, x_{N-1}$, where $x_{n+1} = \varphi x_n$, $-K' \leq n \leq (N-1)$, with $x_{-K'}$ chosen μ -a.e.
2. Obtain, at each point x_n , the unit tangent vector to the unstable manifold, q_n . The following procedure converges exponentially in n to the true value of q_n . Solve the homogeneous tangent equation with repeated normalization. That is, solve

$$(4.5) \quad \alpha_{n+1} q_{n+1} = (d\varphi)_n q_n, \quad n = -K', \dots, 0, 1, \dots,$$

with q_0 being set to a random vector in \mathbb{R}^m , and $\alpha_{n+1} = \|(d\varphi)_n q_n\|$.

3. Solve for v_n the following inhomogeneous tangent equation, which repeatedly projects v_n out of the unstable subspace,

$$(4.6) \quad v_{n+1} = (d\varphi)_n v_n + \chi_{n+1} - a_{n+1} q_{n+1}, \quad n = -K', \dots, 0, 1, \dots,$$

where a_{n+1} is such that $v_{n+1} \cdot q_{n+1} = 0$. The initial condition $v_{-K'}$ is set to $0 \in \mathbb{R}^m$. This equation is henceforth called the *regularized* tangent equation. The error in the solutions v_n when compared to the true value of the vector field v (Theorem 4.1) decreases exponentially with n (as shown in Lemma 8.6).

4. Solve the following second-order tangent equation for p_n , starting with $p_{-K'} = 0 \in \mathbb{R}^m$,

$$(4.7) \quad p_{n+1} = \frac{(d^2\varphi)_n(q_n, q_n) + (d\varphi)_n p_n}{\alpha_{n+1}^2}, \quad n = -K', \dots, 0, 1, \dots,$$

The solutions p_n converge exponentially with n to the true values of the vector field p along the orbit (Lemma 8.7).

5. Solve the following recursive second-order tangent equation for y_n , for each $n \in \mathbb{Z}^+$,

$$(4.8) \quad y_{n+1} = \frac{(d^2\varphi)_n(q_n, v_n) + (d\varphi)_n y_n}{\alpha_{n+1}} + (d\chi)_{n+1} q_{n+1} - c_{n+1} q_{n+1} - a_{n+1} p_{n+1}, \quad n = -K', \dots, 0, \dots,$$

where the scalar c_{n+1} is found using the relationship $y_{n+1} \cdot q_{n+1} = -v_{n+1} \cdot p_{n+1}$. This relationship follows from taking the unstable derivative of $v_{n+1} \cdot q_{n+1} = 0$. The y_n and c_n computed using this procedure also converge exponentially with n to their true values, as shown in Lemma 8.10 and 8.11 respectively.

6. Compute the unstable contribution as the following ergodic average:

$$(4.9) \quad \langle J, \partial_s \mu_s \rangle^u \approx -\frac{1}{N} \sum_{k=0}^{K-1} \sum_{n=0}^{N-1} J_{n+k} c_n.$$

7. Compute the stable contribution as the following ergodic average:

$$(4.10) \quad \langle J, \partial_s \mu_s \rangle^s \approx \frac{1}{N} \sum_{n=0}^{N-1} (dJ)_n \cdot v_n.$$

8. The output of the S3 algorithm is the sum of the stable and unstable contributions, $\langle J, \partial_s \mu_s \rangle^u + \langle J, \partial_s \mu_s \rangle^s$.

The following theorem establishes the convergence of the above S3 algorithm.

Theorem 4.3. *The ergodic averages in Eq. 4.9 and Eq. 4.10 converge to the unstable and stable contributions respectively. In particular,*

1. *for μ -a.e. x_0 and for almost every q_0 ,*

$$(4.11) \quad \langle J, \partial_s \mu_s \rangle^u = -\lim_{K \rightarrow \infty} \lim_{N \rightarrow \infty} \sum_{k=0}^{K-1} \frac{1}{N} \sum_{n=0}^{N-1} J_{n+k} c_n;$$

2. *And, for μ -a.e. x_0 ,*

$$(4.12) \quad \langle J, \partial_s \mu_s \rangle^s := \lim_{N \rightarrow \infty} \frac{1}{N} \sum_{n=0}^{N-1} (dJ)_n \cdot v_n.$$

We prove Theorem 4.3 in section 9. The efficiency of the S3 algorithm in comparison to a direct evaluation of Ruelle's formula (Eq. 3.11) stems from the following. The integrand in Ruelle's original series increases in norm exponentially with k . This makes the ergodic averaging approximation of the integral computationally inefficient, as we noted in section 3.9. By contrast, the norm of the integrand in the S3 modification of the formula (Eq. 4.3) is uniformly bounded in both the stable and unstable contributions. Thus, efficient ergodic-averaging approximations are possible for the S3 formula (Eq. 4.3).

5. Derivation and computation of the S3 formula. In this section and the next, we describe the S3 decomposition of Ruelle’s formula (Eq. 4.2), the derivation of its regularized form (Eq. 4.3), and the computation of the latter. In order to derive an efficient computation of Ruelle’s formula, we split Ruelle’s formula into two parts, using a particular decomposition of the vector field. The contribution to the overall sensitivity made by the unstable component, which is aligned with q , is called the unstable contribution; the remaining term is the stable contribution (Eq. 4.2).

However, we do not decompose χ into its stable and unstable components. That is, although $aq \in E^u$ clearly, a is not chosen such that $\chi - aq$ belongs to E^s . Instead, the scalar field a is chosen so as to be differentiable on the unstable manifold and such that both the stable and unstable contributions lead to well-conditioned computations. The significance of the differentiability of a on the unstable manifold will be clear in the derivation below.

5.1. Regularizing tangent equation solutions. The S3 decomposition can be motivated as a means of regularizing the solutions of a conventional tangent equation. Fixing a reference orbit $\{x_n\}_{n \in \mathbb{Z}^+}$, consider the conventional tangent equation (Eq. 3.2), which is a recursive equation for $u_n := (\partial_s \varphi_s^n)(x_0, s)$, starting from $u_0 = 0 \in \mathbb{R}^m$. As noted in section 3.2, this equation gives the evolution of a tangent vector corresponding to the parameter perturbation along a fixed trajectory, $\{x_n\}_{n \in \mathbb{Z}^+}$. By construction (Eq. 3.2), we can see that $u_n = \sum_{k=0}^{n-1} (d\varphi^k)_{n-k} \chi_{n-k}$. By definition of chaos (section 3.3), $\|d\varphi_x^k \chi_x\| \sim \mathcal{O}(e^{\lambda_1 k})$, for almost every $x \in M$, and almost every perturbation $\chi_x \in \mathbb{R}^m$. Hence, for large n , $\|u_n\| \sim \mathcal{O}(e^{\lambda_1 n})$ for almost every perturbation χ . On the other hand, if we projected out the unstable component of the tangent solution at each timestep, the solution does not exhibit exponential growth. That is, the following iteration is stable

$$(5.1) \quad v_{n+1} = (d\varphi)_n v_n + (\chi_{n+1} - a_{n+1} q_{n+1}),$$

where a_{n+1} is such that $v_{n+1} \cdot q_{n+1} = 0$, for all $n \in \mathbb{Z}^+$. That is, the solution v_n of the above tangent equation along with the repeated projections out of the unstable subspace, is in $E_{x_n}^{u\perp}$ at each n . We refer to the solutions $\{v_n\}$ as *regularized tangent solutions*. With this stable iterative procedure as the motivation, we derive a splitting of Ruelle’s formula. One part of the split formula – the stable contribution – will be computed using the regularized tangent solution, Eq. 5.1.

5.2. Alternative expression of the stable contribution. In the regularized tangent equation (Eq. 5.1), a tangent vector is projected out of the unstable subspace at every iteration. At every $x \in M$, we introduce the orthogonal projection operator, \mathcal{P}_x , to refer to this operation.

Notation 5.1. Let $\mathcal{P}_x : T_x M \rightarrow T_x M$ denote the linear operator that projects a tangent vector onto the hyperplane orthogonal to E_x^u . If q_x is a unit vector in E_x^u , then for any $v_x \in T_x M$, $\mathcal{P}_x v_x := (I - q_x q_x^T) v_x$. Applying \mathcal{P}_x to every point on M would result in a linear operator, hereafter denoted \mathcal{P} , on vector fields of M .

Using this notation, we can reproduce the operations performed by solving Eq. 5.1, by considering a sequence of vector fields $\{v^n\}$ that satisfies the following recurrence relation,

$$(5.2) \quad v^{n+1} = \mathcal{P}(d\varphi v^n + \chi), \quad n \in \mathbb{Z}^+.$$

We also introduce a sequence of scalar fields which denote the components on the unstable subspace that are projected out every iteration. That is, let $\{a^n\}$ be a sequence of scalar fields given by,

$$(5.3) \quad a^{n+1} := q^T(d\varphi v^n + \chi).$$

In Lemma 8.6, we show that the sequence $\{v^n\}$ converges uniformly, starting from any bounded vector field v^0 ; the limit of this sequence is denoted v . The uniform convergence of $\{v^n\}$ implies the uniform convergence of the scalar field $\{a^n\}$, as we show in Lemma 8.8; the limit of this sequence is denoted a . Using these results and uniform hyperbolicity, we prove the following alternative formula for the stable contribution in Proposition 9.1:

$$(5.4) \quad \begin{aligned} \langle J, \partial_s \mu_s \rangle^s &:= \lim_{K \rightarrow \infty} \sum_{k=0}^{K-1} \langle d(J \circ \varphi^k) \cdot (\chi - a^{K-k} q), \mu \rangle \\ &= \langle dJ \cdot v, \mu_s \rangle. \end{aligned}$$

5.3. Computation of the stable contribution. That is, the series summation representing the stable contribution is simply an ensemble average of $dJ \cdot v$, an inner product of two bounded vector fields. That is, for x_0 chosen μ -a.e.,

$$(5.5) \quad \langle J, \partial_s \mu_s \rangle = \lim_{N \rightarrow \infty} \frac{1}{N} \sum_{n=0}^{N-1} (dJ)_n \cdot v_n.$$

The values of the vector field v along the reference orbit are approached by the regularized tangent solution (Eq. 5.1). Without loss of generality, we effect starting the recursive Eq. 5.2 from a zero vector field, by choosing $v_{-K'} = 0 \in \mathbb{R}^m$, at the point $x_{-K'}$. For a large run-up time K' , the solution at 0, v_0 and a_0 are already close to the true values of v and a at x_0 . The solutions thus produced by long-time evolution of the regularized tangent equation (Eq. 5.1) become exponentially more accurate, and are used to evaluate the stable contribution as per Eq. 5.5. In practice, we solve the regularized tangent equation (Eq. 5.1) over an orbit of a long but finite length N . This computes an approximation of the limit on the right hand side up to a finite N . Proposition 9.1 shows that such a computation of the stable contribution converges to its true value (Eq. 5.4) as $N \rightarrow \infty$; the asymptotic error convergence is as $\mathcal{O}(1/\sqrt{N})$.

5.4. Alternative expression of the unstable contribution. Recall that the unstable contribution is the sensitivity due to the perturbation along the unstable subspace,

$$(5.6) \quad \langle J, \partial_s \mu_s \rangle^u = \lim_{K \rightarrow \infty} \sum_{k=0}^{K-1} \langle d(J \circ \varphi^k) \cdot a^{K-k} q, \mu \rangle.$$

As noted in section 3.9, the integrand in the k th term of the above series, $d(J \circ \varphi^k) \cdot a^{K-k} q$, increases exponentially in norm with k . Thus, rather than a direct evaluation, we apply integration by parts on the unstable manifold, which moves the derivative away from the time-dependent term $J \circ \varphi^k$.

Before we integrate by parts, we apply disintegration (Eq. 3.10) of the SRB measure to rewrite the unstable contribution,

$$\begin{aligned}
\langle J, \partial_s \mu_s \rangle^u &:= \lim_{K \rightarrow \infty} \sum_{k=0}^{K-1} \langle a^{K-k} d(J \circ \varphi^k) \cdot q, \mu \rangle \\
(5.7) \quad &= \lim_{K \rightarrow \infty} \sum_{k=0}^{K-1} \int_{M/\Xi} \int_{B_x} a^{K-k} \circ \Phi^x(\xi) \frac{d(J \circ \varphi^k \circ \Phi^x)}{d\xi}(\xi) \rho^x \circ \Phi^x(\xi) d\xi d\hat{\mu}(x),
\end{aligned}$$

where $B_x := \Phi^{x^{-1}}(\Xi_x)$. When compared to Eq. 3.10, we have additionally used a change of variables, $x' \rightarrow \xi$, in the inner integral. Since $\|\Phi^{x'}(\xi)\| = 1$, by construction, this change of variables does not introduce a multiplicative factor in the integrand. Now applying integration by parts on the inner integral, the k th term on the right hand side of Eq. 5.7 becomes,

$$\begin{aligned}
&\int_{M/\Xi} \int_{\partial B_x} \frac{d((a^{K-k} J \circ \varphi^k \rho^x) \circ \Phi^x)}{d\xi} d\xi d\hat{\mu}(x) \\
(5.8) \quad &- \int_{M/\Xi} \int_{B_x} J \circ \varphi^k \circ \Phi^x \left(\frac{d(a^{K-k} \circ \Phi^x)}{d\xi} + \frac{a^{K-k} \circ \Phi^x}{\rho \circ \Phi^x} \frac{d(\rho^x \circ \Phi^x)}{d\xi} \right) (\rho^x \circ \Phi^x) d\xi d\hat{\mu}(x).
\end{aligned}$$

The first term in the above equation vanishes due to cancellations on the boundaries of B_x for different x (Theorem 3.1(b) in [53][54]; see also [34]). Changing variables back to x' , we obtain the following regularized expression for the unstable contribution,

$$\begin{aligned}
\langle J, \partial_s \mu_s \rangle^u &= - \lim_{K \rightarrow \infty} \sum_{k < K} \int_{M/\Xi} \int_{\Xi_x} J \circ \varphi^k(x') \left(\frac{d(a^{K-k} \circ \Phi^x)}{d\xi} ((\Phi^x)^{-1}(x')) \right) \\
(5.9) \quad &+ \frac{a^{K-k}(x')}{\rho^x(x')} \frac{d(\rho^x \circ \Phi^x)}{d\xi} ((\Phi^x)^{-1}(x')) \rho^x(x') d\nu_x(x') d\hat{\mu}(x),
\end{aligned}$$

We introduce the logarithmic density gradient function [57][46],

$$(5.10) \quad g^x(x') := \frac{1}{\rho^x(x')} \frac{d(\rho^x \circ \Phi^x)}{d\xi} ((\Phi^x)^{-1}(x')).$$

As we show in section 6.2, g^x does not depend on x , and hence we denote the density gradient simply as g . We also introduce the scalar field sequence b^k defined as $b_x^k := d_\xi(a^k \circ \Phi^x)(0)$ to denote the unstable derivative of a^k , deferring the (constructive) proof of its uniform convergence until Lemma 8.11. This leads us to the following expression for the unstable contribution,

$$(5.11) \quad \langle J, \partial_s \mu_s \rangle^u = - \lim_{K \rightarrow \infty} \sum_{k=0}^{K-1} \langle J \circ \varphi^k (g a^{K-k} + b^{K-k}), \mu \rangle.$$

Recall that we compute a^k iteratively along a typical trajectory as part of the stable contribution computation (section 5.2). We are now left with the computation of g and b^k

along the trajectory. These are tackled in section 6.2 and 6.3 respectively. Ni [46] addresses the computation of the divergence on the unstable manifold (analogous to the function g described above), where the differentiation is performed on a set of *shadowing* coordinates that are tied to the parameter perturbation. This is part of an algorithm to compute linear response that uses a different decomposition from the present paper, into shadowing and unstable directions. However, the shadowing direction, v^{sh} in [46] is related to our regularized tangent vector field v , by the relation $\mathcal{P}v^{\text{sh}} = v$ (see [46] or Appendix A).

6. Computing derivatives along unstable manifolds. In the previous section, we obtained a regularized expression for the unstable contribution. That is, the integrand in the regularized expression, Eq. 5.11, is uniformly bounded – the uniform boundedness of the scalar field sequences $\{a^k\}$ and $\{b^k\}$ and the boundedness of g are proved in Lemma 8.8, 8.11 and 9.2 respectively. The question still remains how we can compute the unknown scalar fields g and b . For both these computations, we require second-order unstable derivatives, which we discuss next.

6.1. Iteratively computing the curvature of the unstable manifold. The function $\Phi^{x'}(\xi)$ is an arclength travelled by a particle on a local unstable manifold of x' , starting from x' . The particle travels with unit speed, and its instantaneous velocity at time ξ is $q_{\Phi^{x'}(\xi)}$. Its acceleration field is given by $w^{x'} := d_\xi^2 \Phi^{x'}(\xi)$. We derive a recursive equation satisfied by this family, by starting with a differentiation with respect to ξ of the definition of α (Eq. 3.6),

$$(6.1) \quad \alpha_{\varphi x}^2 \gamma_{\varphi x}^{\varphi x'} = (d\varphi_x q_x)^T (d\varphi_x w_x^{x'} + d^2\varphi_x(q_x, q_x)).$$

Here $\gamma_x^{x'} := d_\xi(\alpha \circ \Phi^{x'})((\Phi^{x'})^{-1}x)$ is the unstable derivative of α ; $d^2\varphi_x$ is the bilinear form that returns a tangent vector $\in T_{\varphi x}M$; it can be written as an $m \times m \times m$ tensor consisting of component-wise partial derivatives of the Jacobian $d\varphi_x$. In deriving Eq. 6.1, we have used the chain rule in Eq. 3.7. Now differentiating the statement of covariance of the unstable subspace (section 3.4), $\alpha_{\varphi x} q_{\varphi x} = d\varphi_x q_x$,

$$(6.2) \quad \alpha_{\varphi x} \gamma_{\varphi x}^{x'} q_{\varphi x} + \alpha_{\varphi x}^2 w_{\varphi x}^{\varphi x'} = d\varphi_x w_x^{x'} + d^2\varphi_x(q_x, q_x).$$

Substituting Eq. 6.1 into Eq. 6.2, and using the definition of α ,

$$(6.3) \quad w_{\varphi x}^{\varphi x'} = \frac{1}{\alpha_{\varphi x}^2} (I - q_{\varphi x} q_{\varphi x}^T) (d\varphi_x w_x^{x'} + d^2\varphi_x(q_x, q_x)),$$

where I is the $m \times m$ identity matrix. The above equation represents the following relationship between elements of the family of vector fields, $\{w^x\}$,

$$(6.4) \quad w^{\varphi x} = \mathcal{P} \frac{d\varphi w^x + d^2\varphi(q, q)}{\alpha^2}.$$

In Lemma 8.7, we show that any bounded sequence $\{w^n\}$ of vector fields that satisfies,

$$(6.5) \quad w^{n+1} = \mathcal{P} \frac{d\varphi w^n + d^2\varphi(q, q)}{\alpha^2}$$

converges uniformly to a unique vector field w . Hence, the family $\{w^x\}$ does not depend on the parameterization centers, and simply denotes a single vector field, which we call w . Reconsidering Eq. 6.1,

$$(6.6) \quad \gamma_{\varphi x}^{\varphi x'} = \frac{q_{\varphi x}^T}{\alpha_{\varphi x}} (d\varphi_x w_x + d^2\varphi_x(q_x, q_x)),$$

it is clear that the family of scalar fields $\{\gamma^x\}$ is also independent of the parameterization. We henceforth write $\gamma = \partial_\xi \alpha$, to denote the unstable derivative of the scalar field α .

Similarly, the scalar fields $d_\xi(a \circ \Phi^x)$ and $d_\xi(\log \rho^x \circ \Phi^x)$ can be attained as limits of (exponentially) uniformly converging sequences of scalar fields, as proved in Lemma 8.11 and Lemma 9.2 respectively. Thus, by the same argument as we used for $\{w^x\}$, these limits are independent of the parameterization centers and are denoted simply $b := \partial_\xi a$ and $g := \partial_\xi \log \rho^x$ respectively.

The curvature of a local unstable manifold is the magnitude of the acceleration experienced by a particle travelling at unit speed. That is, the curvature of the unstable manifold at x is $\|w_x\|$. From Eq. 6.1, it is clear that the computation of the curvature and that of γ go hand in hand. To compute both w and then using Eq. 6.1, γ , along a typical trajectory, we solve the second-order tangent equation derived above (Eq. 6.5) iteratively along the trajectory. In practice, we assume $w_0^0 := w_{x_0}^0 = 0$ at some μ -typical x_0 and iterate Eq. 6.5. Such a computation converges exponentially with n to the true value of w_n due to Lemma 8.7. At each step of the recursion, the value of γ_n , which is computed through Eq. 6.1 using the computed values of w_n , also becomes exponentially more accurate. These values of γ_n along the orbit $\{x_n\}$ are used to obtain g along the orbit, as we shall discuss in the next subsection.

From Eq. 6.5, we can also infer that the vector field w is orthogonal to q (i.e., the acceleration of a particle on a local unstable manifold is perpendicular to its velocity). Visualizations of the unstable manifold curvatures obtained from the norms of w_n computed as above are shown for classical hyperbolic attractors in [18].

6.2. Iterative formula for unstable derivatives of SRB density. In a previous work [57], we provide an intuitive explanation of the density gradient g as well as its computation in one-dimensional expanding maps of the interval, where the global unstable manifold is the background manifold M . In the present setting of a one-dimensional unstable manifold, we see that our derivation leads to a similar computation of g as in 1D expanding maps. From our expression for the SRB density (Eq. 3.3), we find that for $x \in \Xi_{x'}$,

$$(6.7) \quad \rho_x^{x'} = \rho_{\varphi^{-1}x}^{\varphi^{-1}x'} \frac{\alpha_{x'}}{\alpha_x} \frac{\bar{\rho}^{\varphi^{-1}x'}}{\bar{\rho}^{x'}}.$$

We recall that phase points appearing on superscripts indicate the centers of our coordinate system Φ^x (section 3.6), while on subscripts, they indicate evaluations of the function (e.g., in Eq. 6.7, the scalar functions $\rho^{x'}$ and $\rho^{\varphi^{-1}x'}$ are evaluated at x and $\varphi^{-1}x$ respectively). Taking logarithm and differentiating Eq. 6.7 with respect to ξ on the unstable manifold at x , using

the definition (Eq. 5.10) of the density gradient g^x ,

$$\begin{aligned} g_x^{x'} &= \frac{g_{\varphi^{-1}x}^{\varphi^{-1}x'}}{\alpha_x} - \frac{1}{\alpha_x} \frac{d(\alpha \circ \Phi^{x'})}{d\xi}((\Phi^{x'})^{-1}(x)) \\ (6.8) \quad &= \frac{g_{\varphi^{-1}x}^{\varphi^{-1}x'}}{\alpha_x} - \frac{\gamma_x}{\alpha_x}. \end{aligned}$$

To derive the first term on the right hand side, we have also used the chain rule for our parameterization (Eq. 3.7) and the scalar field γ introduced in the previous subsection. Now, in Lemma 9.2, we show that starting from any bounded scalar function h^0 , and considering any bounded function r , the following recursion converges uniformly,

$$(6.9) \quad h_{\varphi x}^{n+1} = \frac{h_x^n}{\alpha_{\varphi x}} + r_{\varphi x}.$$

Since the sequence of functions $\{g^{\varphi^n x}\}_{n=-\infty}^0$ in Eq. 6.8 satisfies this same recursion, the family of functions $\{g^x\}$ must indeed be a single function independent of x . Hence, we omit the superscript x , and simply denote the density gradient g . Thus, Eq. 6.8 can be rewritten as follows, fixing some μ -typical reference orbit $\{x_n\}$:

$$(6.10) \quad g_{n+1} = \frac{g_n}{\alpha_{n+1}} - \frac{\gamma_{n+1}}{\alpha_{n+1}}.$$

This iterative equation exponentially converges (Lemma 9.2), with n , to the true value of $g_n := g(x_n)$, along almost every orbit. In practice, we start the computation with an arbitrary initialization.

6.3. Iterative computation of the scalar field b . Having completely prescribed a computation for g , the only unknown we are left with in computing the unstable contribution (Eq. 5.11) is the scalar field b . We describe a procedure, involving w , and a new second-order tangent equation. This latter second-order tangent solution exponentially approaches the vector field representing the unstable derivative of v . In order to derive this equation, recall that the vector field v is the limit of a sequence $\{v^n\}$ described in Eq. 5.2. The sequence $\{v^n\}$ is differentiable in the unstable direction, if we start with a differentiable vector field v^0 . In Lemma 8.10, we show that the sequence of these derivatives, denoted $\{y^n\}$, converges uniformly. Since $\{v^n\}$ also converges uniformly, the limit y of the sequence $\{y^n\}$ is the unstable derivative of v .

Thus, it is valid to differentiate the regularized tangent equation (Eq. 5.1) in the unstable direction. Taking this derivative, we obtain that the vector field y satisfies the following equation, along a fixed μ -typical orbit $\{x_n\}_{n \in \mathbb{Z}^+}$

$$(6.11) \quad \begin{aligned} \alpha_{n+1}y_{n+1} &= (d\varphi)_n y_n + (d^2\varphi)_n(q_n, v_n) \\ &+ \alpha_{n+1}(d\chi)_{n+1} q_{n+1} - \alpha_{n+1}b_{n+1}q_{n+1} - \alpha_{n+1}a_{n+1}w_{n+1}. \end{aligned}$$

As usual, we have used the chain rule for differentiating on unstable manifolds (Eq. 3.7) and the differentiability of $d\varphi$ and χ on M . We have suppressed the parameterization centers on

the superscripts because the unstable derivatives y and b are limits of uniformly converging series, and hence we can invoke the same argument as in sections 6.1 and 6.2 to show their independence from the parameterization. Using Lemma 8.10, we can argue that the iteration above converges to the true value of the vector y_n as $n \rightarrow \infty$, starting with an arbitrary value for y_0 . In order to compute the above recursion, we must know the value of b along the trajectory. However, it is possible to close this system of equations for y_{n+1} and b_{n+1} by differentiating in the unstable direction, the definition of a_{n+1} .

Recall that the regularized tangent solutions v_n are orthogonal to q_n and a_n are chosen so as to enforce this orthogonality. From Eq. 5.1, we get,

$$(6.12) \quad a_{n+1} = q_{n+1} \cdot ((d\varphi)_n v_n + \chi_{n+1}).$$

Differentiating the above equation in the unstable direction,

$$(6.13) \quad \begin{aligned} \alpha_{n+1} b_{n+1} &= ((d^2\varphi)_n(v_n, q_n) + (d\varphi)_n y_n + \alpha_{n+1}(d\chi_{n+1} q_{n+1})) \cdot q_{n+1} \\ &+ \alpha_{n+1} w_{n+1} \cdot ((d\varphi)_n v_n + \chi_{n+1}). \end{aligned}$$

By comparing Eq. 6.13 with the inner product of Eq. 6.11 with q_{n+1} , we see that

$$(6.14) \quad y_{n+1} \cdot q_{n+1} = -w_{n+1} \cdot ((d\varphi)_n v_n + \chi_{n+1}).$$

By using the orthogonality $w_{n+1} \cdot q_{n+1} = 0$, which follows from Eq. 6.3, on Eq. 5.1, we obtain $w_{n+1} \cdot v_{n+1} = w_{n+1} \cdot ((d\varphi)_n v_n + \chi_{n+1})$. Thus, we can further simplify Eq. 6.14 to obtain the constraint,

$$(6.15) \quad y_{n+1} \cdot q_{n+1} = -w_{n+1} \cdot v_{n+1}.$$

Thus, we have two equations (Eq. 6.11 and Eq. 6.15) from which the two unknowns b_{n+1} and y_{n+1} are solved for. Without loss of generality, we start the iteration in Eq. 6.11 with $y_0 = 0 \in \mathbb{R}^m$. Then, by Lemma 8.10 and Lemma 8.11, this iterative procedure yields exponentially accurate values of both y_n and b_n along a trajectory.

6.4. Computation of the unstable contribution. We now assemble the components computed in the previous subsections together to form the unstable contribution, which we recall from Eq. 5.11,

$$(6.16) \quad \langle J, \partial_s \mu_s \rangle^u = - \lim_{K \rightarrow \infty} \sum_{k=0}^{K-1} \langle J \circ \varphi^k (a^{K-k} g + b^{K-k}), \mu \rangle.$$

Recall that, by increasing the run-up time K' , the scalar fields a^k and b^k , $k \geq 0$, become arbitrarily close in the supremum norm, to a and b respectively. In addition, we shall assume a strong form of exponential correlation decay (section 3.5) by which, for a Hölder continuous field l with $\langle l, \mu \rangle = 0$, there exists a $c_l > 0$ such that $|\langle (J \circ \varphi^n) l, \mu \rangle| \leq c_l \lambda^n \|l\|$, for all n . Under this assumption, with $l = (a^{K-k} - a)g + (b^{K-k} - b)$,

$$(6.17) \quad \left| \sum_{k=0}^{K-1} \left(\langle J \circ \varphi^k (a^{K-k} g + b^{K-k}), \mu \rangle - \langle J \circ \varphi^k (ag + b), \mu \rangle \right) \right| \leq \|g\| c_3 c_1 K \lambda^K + c_4 c_2 K \lambda^K,$$

because there exist constants $c_1, c_2 > 0$ such that $\|a^{K-k} - a\| \leq c_1 \lambda^{K-k}$ and $\|b^{K-k} - b\| \leq c_2 \lambda^{K-k}$ according to Lemmas 8.8 and 8.11 respectively. Letting $K \rightarrow \infty$, we conclude that the unstable contribution may be computed as

$$(6.18) \quad \langle J, \partial_s \mu_s \rangle^u = - \sum_{k=0}^{\infty} \langle J \circ \varphi^k (ag + b), \mu \rangle.$$

In practice, we need only a small number K of terms in the series above to approximate the unstable contribution to within a given tolerance. We fix some N -length μ -typical orbit $\{x_n\}$ along which we compute the first K terms above,

$$(6.19) \quad \langle J, \partial_s \mu_s \rangle^u \approx - \sum_{k=0}^{K-1} \frac{1}{N} \sum_{n=0}^{N-1} J_{n+k} (a_n g_n + b_n).$$

This computation, due to decay of correlations, converges as $N \rightarrow \infty$ and $K \rightarrow \infty$, in that order. Further, the error in approximating each term of Eq. 6.16 as an N -time ergodic average declines as $\mathcal{O}(1/\sqrt{N})$, up to a factor iterated logarithmic in N . A complete discussion of the error convergence of the unstable contribution computation is deferred until section 9.2.2, after the proofs of convergence of the individual computational components of Eq. 6.19. Here we remark that even if the equivalence between Eq. 6.18 and the unstable contribution (Eq. 6.16) does not strictly hold, the error in approximating the unstable contribution (Eq. 6.16) by Eq. 6.19 becomes negligible for a sufficiently long run-up time K' (section 4.1). This is because, for large K' , $a^k, 0 \leq k \leq K-1$ are all approximately equal to a and $b^k, 0 \leq k \leq K-1$ are all approximately equal to b , due to Lemmas 8.8 and 8.11 respectively.

Now we summarize these individual components that lead to the computation of the unstable contribution by Eq. 6.19. Let $\{x_n\}_{n=-K'}^{N-1}$ be a sufficiently long finite-length μ -typical orbit. In order to compute Eq. 6.19, we need the values of a, b and g along the orbit. First, we note that the (approximate) values of a along the orbit are known from the regularized tangent solution (Eq. 5.1),

$$(6.20) \quad a_{n+1} = q_{n+1}^T ((d\varphi)_n v_n + \chi_{n+1}).$$

In section 6.2, we derived a recursive equation for the density gradient function,

$$(6.21) \quad g_{n+1} = \frac{g_n}{\alpha_{n+1}} - \frac{\gamma_{n+1}}{\alpha_{n+1}},$$

which we begin by arbitrarily setting $g_{-K'} = 0$. The scalar field γ , which denotes the unstable derivative of the expansion factor α , is evaluated along an orbit by solving for the vector field w (section 6.1). Summarizing this step here, the recursive formula

$$(6.22) \quad w_{n+1} = \frac{1}{\alpha_{n+1}^2} (I - q_{n+1} q_{n+1}^T) ((d\varphi)_n w_n + (d^2\varphi)_n(q_n, q_n))$$

is again started with the arbitrary choice $w_{-K'} \in \mathbb{R}^m$; at each step of the recursion, the values of γ along an orbit are set to

$$(6.23) \quad \gamma_{n+1} = \frac{q_{n+1}^T}{\alpha_{n+1}} ((d\varphi)_n w_n + (d^2\varphi)_n(q_n, q_n)).$$

Finally, the values b_n are obtained simultaneously with y_n from Eq. 6.11 and Eq. 6.15, which are repeated here for clarity:

$$(6.24) \quad \begin{aligned} y_{n+1} &= \frac{(d\varphi)_n y_n + (d^2\varphi)_n(q_n, v_n)}{\alpha_{n+1}} \\ &+ (d\chi)_{n+1} q_{n+1} - b_{n+1} q_{n+1} - a_{n+1} w_{n+1}, \end{aligned}$$

where b_{n+1} is such that $y_{n+1} \cdot q_{n+1} = -v_{n+1} \cdot w_{n+1}$, at each n . Using the values of a_n , b_n and g_n obtained approximately, as outlined above, we compute an N -sample average of the k -lag correlation with J , in order to compute the k th term of the unstable contribution (Eq. 6.19). Putting this together with the stable contribution (Eq. 5.5), we obtain the overall sensitivity. These steps are condensed into the S3 algorithm listed in section 4.1, with one simplification: we can eliminate the need to compute Eq. 6.21 explicitly. To see this, let us consider Eq. 6.22 without the projection,

$$(6.25) \quad \begin{aligned} p_{n+1} &= \frac{1}{\alpha_{n+1}^2} ((d\varphi)_n p_n + (d^2\varphi)_n(q_n, q_n)) \\ p_{-K'} &= 0 \in \mathbb{R}^m. \end{aligned}$$

Using these solutions p_n , Eq. 6.23 and Eq. 6.21, we find that

$$a_{n+1} w_{n+1} = a_{n+1} g_{n+1} q_{n+1} + a_{n+1} p_{n+1}.$$

Substituting this relationship into Eq. 6.24 leads to

$$(6.26) \quad \begin{aligned} y_{n+1} &= \frac{(d\varphi)_n y_n + (d^2\varphi)_n(q_n, v_n)}{\alpha_{n+1}} + (d\chi)_{n+1} q_{n+1} \\ &- c_{n+1} q_{n+1} - a_{n+1} p_{n+1}, \end{aligned}$$

where $c_{n+1} := (a_{n+1} g_{n+1} + b_{n+1})$. Notice that we only need the scalar field c , and not b and g explicitly, to compute the unstable contribution and since by iterating Eq. 6.26 we obtain c_n directly, we avoid computing g via Eq. 6.21. Since the above equation replaces the use of w_n with p_n , we do not need to solve for w_n through Eq. 6.22 either; rather, we just compute p_n by iterating Eq. 6.25. Although we used w_n in the constraint (Eq. 6.14) needed to solve for b_n , and now c_n , the constraint may be rewritten using p_n as,

$$(6.27) \quad y_{n+1} \cdot q_{n+1} = -v_{n+1} \cdot w_{n+1} = -v_{n+1} \cdot p_{n+1}.$$

The second equality is true because p_{n+1} is of the form $w_{n+1} + \delta_{n+1} q_{n+1}$, for some scalar sequence $\{\delta_{n+1}\}$, and $v_{n+1} \cdot q_{n+1} = 0$ by construction (Eq. 5.1).

7. Numerical results.

7.1. Perturbations of the Baker's map. In order to validate the S3 algorithm, we consider perturbations of the standard Baker's map that are designed to elicit both stable and unstable

contributions. Consider the following self-map φ_s of the torus \mathbb{T}^2 , where $s = [s_1, s_2, s_3, s_4]^T \in \mathbb{R}^4$,

$$(7.1) \quad \varphi_s([x^{(1)}, x^{(2)}]^T) = \left[\frac{2x^{(1)} + (s_1 + s_2 \sin(2x^{(2)}/2)) \sin x^{(1)} - \lfloor x^{(1)}/\pi \rfloor 2\pi}{x^{(2)} + (s_4 + s_3 \sin x^{(1)}) \sin(2x^{(2)}) + \lfloor x^{(1)}/\pi \rfloor \pi} \right] \bmod 2\pi.$$

The standard Baker's map is recovered at $s = 0 \in \mathbb{R}^4$. We isolate the effect of each parameter by illustrating the action of perturbed maps with all except one parameter set to 0. Figure 1 elucidates the effect of s_1 and s_2 . The unperturbed Baker's map, as shown in Figure 1 (top right), uniformly expands in the horizontal direction ($\hat{x}^{(1)}$) and contracts in the vertical direction ($\hat{x}^{(2)}$). By contrast, when the parameter s_1 is non-zero (and the other parameters are set to 0), the expansion in the $\hat{x}^{(1)}$ direction depends on $x^{(1)}$, resulting in a non-uniformly expanded grid as shown on the bottom left of Figure 1. On the bottom right of Figure 1, we show the effect of the parameter s_2 , from which it is clear that the expansion in the $\hat{x}^{(1)}$ direction depends nonlinearly on the $x^{(2)}$ coordinate.

In Figure 2 (top right), the expansion and contraction by constant factors, in the $\hat{x}^{(1)}$ and $\hat{x}^{(2)}$ directions respectively, by the unperturbed map, are clearly seen from the uniform stretching and contraction of the horizontal strips on the top left. On the bottom row, the effect of the parameters s_3 and s_4 , acting in isolation, are shown on the left and right respectively. From Eq. 7.1, it is clear that s_3 introduces a nonlinear variation with $x^{(1)}$ in the contraction along the $\hat{x}^{(2)}$ direction. This is indeed reflected in the image of the horizontal strips (top left of Figure 2) under the perturbed map, which is shown on the bottom left of Figure 2. Finally, the bottom right plot shows that the contraction in $\hat{x}^{(2)}$ is nonuniform with respect to the $x^{(2)}$ coordinate but uniform along the $x^{(1)}$ coordinate, as we would expect from Eq. 7.1 with s_4 being the only non-zero parameter.

7.1.1. Stable and unstable subspaces. The standard Baker's map has uniform stable and unstable subspaces, which are aligned with $\hat{x}^{(2)}$ and $\hat{x}^{(1)}$ respectively, i.e., $E_x^u \equiv \hat{x}^{(1)} = \text{span}\{[1, 0]^T\}$ and $E_x^s \equiv \hat{x}^{(2)} = \text{span}\{[0, 1]^T\}$ at all $x \in M$. The perturbations of s_1 and s_4 do not alter these uniform stable and unstable directions. It can be verified that the perturbation of s_2 alters the stable direction while retaining $\hat{x}^{(1)}$ as the unstable direction everywhere. The perturbed map with s_3 being the only non-zero parameter has a non-uniform unstable subspace that is not parallel to $\hat{x}^{(1)}$ everywhere. On the other hand, its stable subspaces are everywhere parallel to $\hat{x}^{(2)}$.

7.1.2. SRB measures of perturbed Baker's maps. The perturbations of the Baker's map and the original map are all uniformly hyperbolic. Numerical approximations of the SRB measures of the perturbed maps associated to each parameter acting in isolation are shown in Figure 3. Specifically, we plot, on a 400×729 grid of \mathbb{T}^2 , the empirical distributions computed using a long orbit (of length 1.6 trillion), say $\{x_n\}_{-K \leq n \leq N}$, where x_0 can be assumed to sample the SRB measure, for a large enough K . At each grid cell $A \subset (0, 2\pi)^2$ we calculate the empirical probability, $\mu_{\text{emp}}^N(A) = (1/N) \sum_{n=0}^{N-1} 1_A(x_n)$, where 1_A , defined as $1_A(x) = 1$ when $x \in A$ and 0 otherwise, is the indicator function on the set A . Since the SRB measure is physical, $\mu_{\text{emp}}^N(A) \rightarrow \mu(A)$ as $N \rightarrow \infty$. The colorbar in Figure 3 indicates the value $\mu_{\text{emp}}^N(A)/\text{mean}(\mu_{\text{emp}}^N)$, where $\text{mean}(\mu_{\text{emp}}^N)$ is the sample mean over all grid cells. We

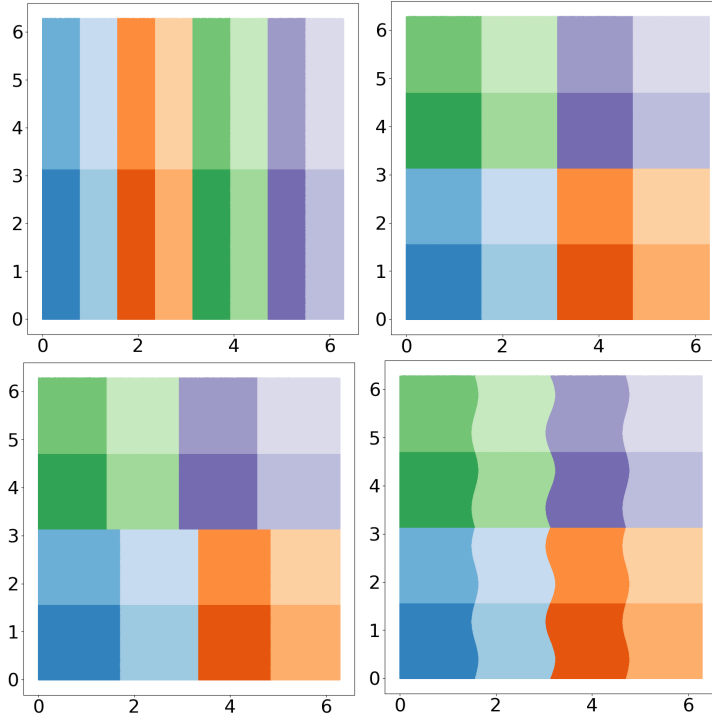


Figure 1. Top left: the domain \mathbb{T}^2 covered by rectangles. The other figures show the application of Baker's map at $s = 0 \in \mathbb{R}^4$ (top right), $s = [0.2, 0, 0, 0]^T$ (bottom left) and $s = [0, 0.2, 0, 0]$ (bottom right) on the gridded top left figure.

verify that upon increasing the number of grid cells, $\mu_{\text{emp}}^N(A)/(\text{area}(A))$ also increases. This numerical observation supports the lack of absolute continuity of μ with respect to Lebesgue. In particular, we observe that the empirical distributions are supported on Cantor-like sets in the $\hat{x}^{(2)}$ direction, which is the stable direction in all cases except the s_2 perturbation. That is, when the number of grid cells along $\hat{x}^{(2)}$ is 3^k we observe that about 2^k of them are not visited by the orbit.

To summarize, while the SRB measure of the unperturbed Baker's map ($s = 0 \in \mathbb{R}^4$) is the Lebesgue measure on \mathbb{T}^2 , the perturbed maps have SRB measures that are not absolutely continuous with respect to Lebesgue on \mathbb{T}^2 . This is visually observed in Figure 3, where, in every case, the distribution appears to have fractal support in the $\hat{x}^{(2)}$ direction. The SRB distribution in each case is absolutely continuous on the unstable manifold, which is uniform and parallel to $\hat{x}^{(1)}$ in every case except the s_3 perturbation. In the perturbed map with s_3 being non-zero (bottom left of Figure 3), the SRB measure appears smooth along its curved unstable manifold, and rough along its stable manifold, which is uniform and parallel to the $\hat{x}^{(2)}$ direction. As noted in section 7.1.1, while the unstable manifold of the perturbed map with $s_2 \neq 0$ is parallel to $\hat{x}^{(1)}$ everywhere, the stable manifold is curved around the $\hat{x}^{(2)}$ direction. This picture is consistent with smoothness of the map's SRB measure (top right of Figure 3) in the $\hat{x}^{(1)}$ direction and the lack of smoothness in the vertical direction, which appears distinct from the s_4 case where the stable manifold is uniformly parallel to the $\hat{x}^{(2)}$

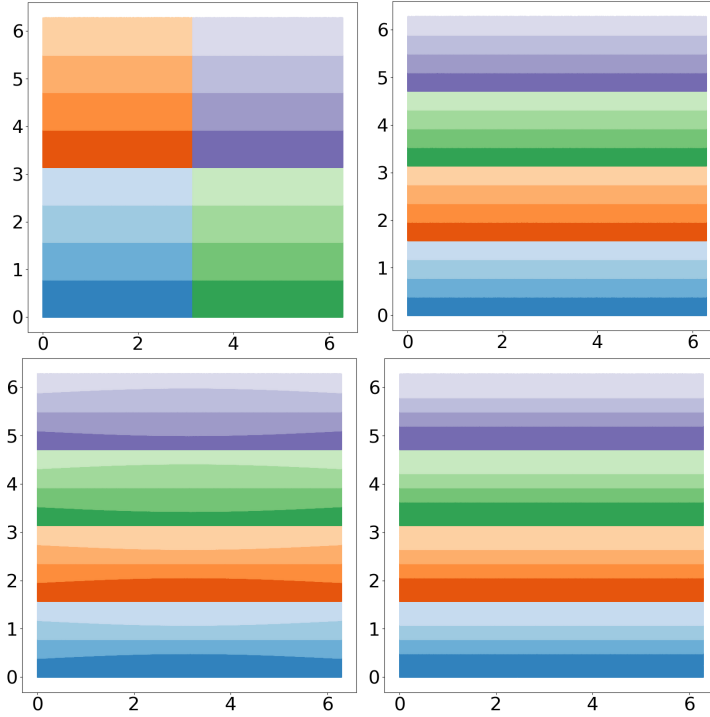


Figure 2. Top left: the domain \mathbb{T}^2 covered by rectangles. The other figures show the application of Baker's map at $s = 0 \in \mathbb{R}^4$ (top right), $s = [0, 0, 0.2, 0]^T$ (bottom left) and $s = [0, 0, 0, 0.2]$ (bottom right) on the gridded top left figure.

direction.

7.1.3. Sensitivities of a smooth objective function. We make an arbitrary choice of a smooth objective function, $J([x^{(1)}, x^{(2)}]^T) = \cos 4x^{(2)}$, and validate the parametric derivatives of its statistics computed by S3 in each perturbed Baker's map. The validation results are shown in Figures 4 and 5. In the left plot of Figure 4, only perturbations of s_1 are considered, while other parameters are held at 0. This leads to only an unstable contribution to the sensitivity because $\chi_{\varphi_{s_1} x} = [\sin x^{(1)} \ 0]^T$ which is aligned with the unstable direction $\hat{x}^{(1)} = [1 \ 0]^T$ at all x . The ergodic/ensemble averages of J are shown as a function of s_1 in blue; superimposed as black lines are the linearly extrapolated values of the S3 sensitivities computed at many different values of s_1 . We see that the derivatives of the $\langle J \rangle$ vs. s_1 are closely approximated by S3. This validates the computation of sensitivities to unstable perturbations by S3.

Similarly, we show the validation of the S3 algorithm to stable perturbations, on the right plot of Figure 4. To generate these plots, ergodic/ensemble averages of J are computed at perturbed maps where only s_4 is varied. In this case, χ is aligned with $\hat{x}^{(2)}$, which is the uniform stable direction. The S3 sensitivities, shown in black, are perfectly tangent to the response curves $\langle J \rangle$ vs. s_4 , as shown in Figure 4 (right).

To test S3 on maps with non-uniform stable and unstable directions, we apply the algorithm to compute linear response in maps with non-zero s_2 and s_3 . At a non-zero s_2 parameter, when all other parameters are held at 0, the stable manifold is non-uniform, while

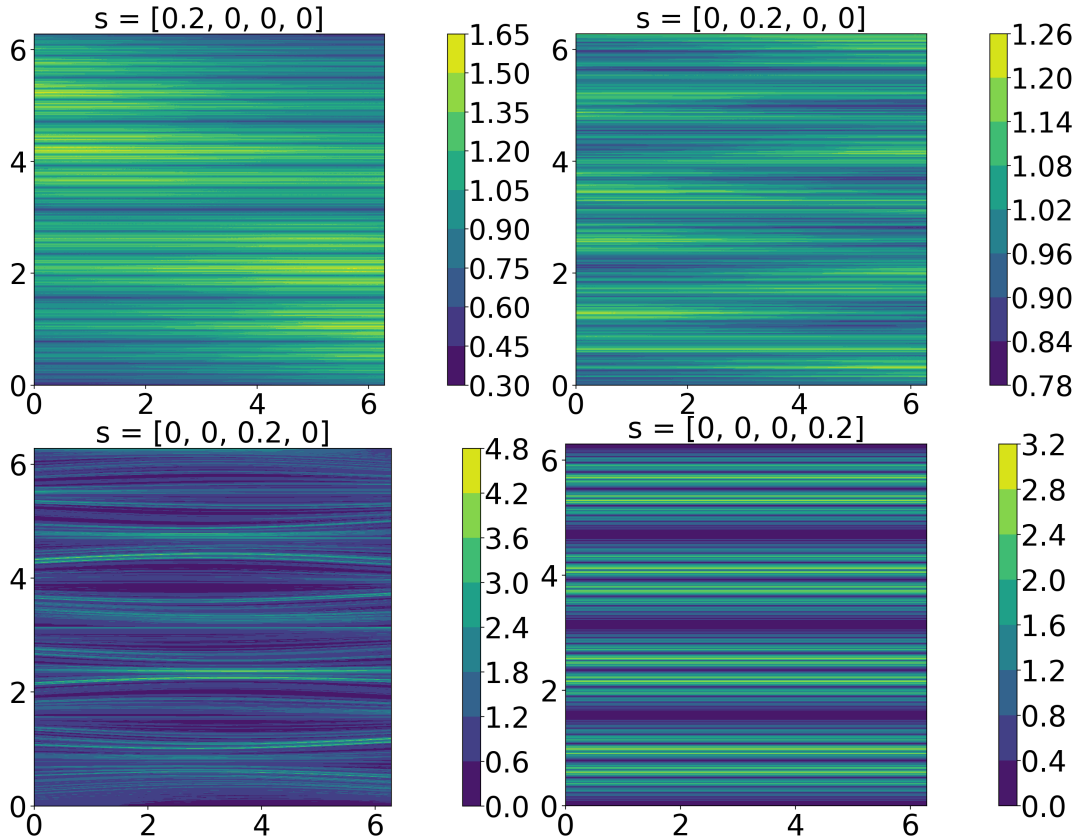


Figure 3. Each plot shows a scaled SRB distribution achieved at the parameter values indicated on the title. A histogram of an orbit of length of 1.6 trillion is computed on a 400×729 grid. The histogram values are scaled by their mean over all grid cells.

the unstable manifold is uniform and tangent to $\hat{x}^{(1)}$. The overall sensitivity contains only an unstable contribution, which is verified to be correct in Figure 5 (left). As a final test, we put $s_1 = s_3$ and vary this parameter, which makes the unstable manifold curved and nonuniform. The response curves are shown (in blue) in Figure 5, on which the S3 sensitivities (black), which have both non-zero stable and unstable contributions, are plotted. Once again, the S3 derivatives are accurate over a range of parameter values. In each case, we chose $K = 11$ (terms summed in Ruelle's series) and $N = 500000$ (samples to compute ergodic averages), in the S3 algorithm; the blue points in each figure were ensemble averages over 160 million samples.

7.2. Perturbations of the Solenoid attractor. Next we consider the classical uniformly hyperbolic example of the Smale-Williams Solenoid map. We introduce a set of parameters $s = [s_1, s_2]^T$, which takes the reference value $[1, 0]^T$. The perturbed Smale-Williams Solenoid

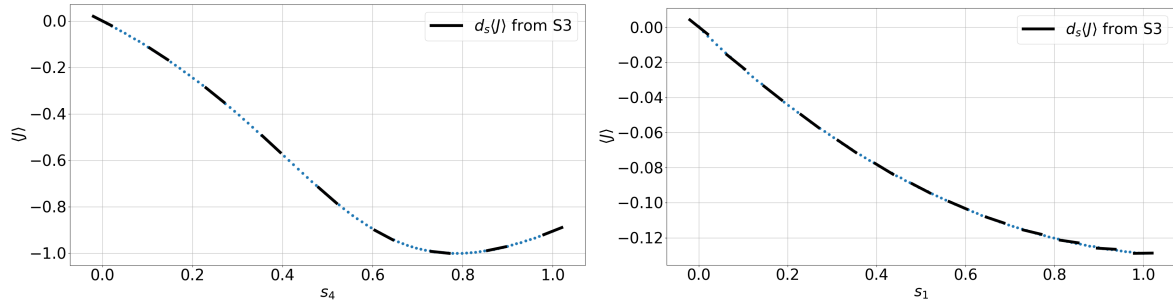


Figure 4. Ergodic average of the objective function $J = \cos(4x_2)$ as a function of s_4 (left) and s_1 (right); the other parameters are set to 0. Sensitivities from $S3$ are shown in black at select parameter values.

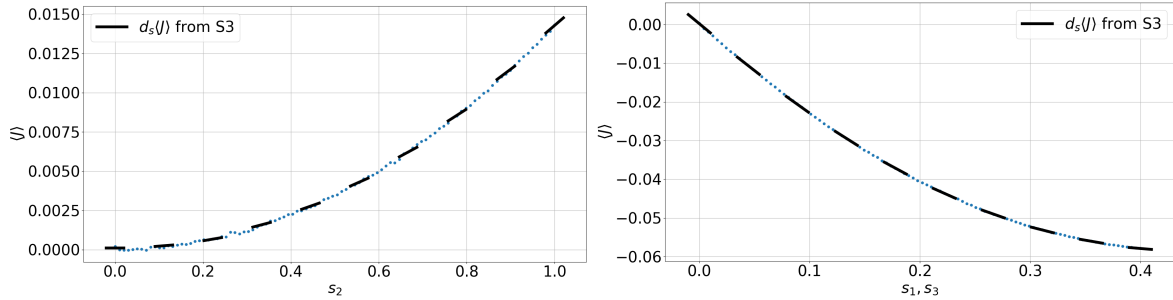


Figure 5. Ergodic average of the objective function $J = \cos(4x_2)$ as a function of s_4 (left) and $s_1 = s_3$ (right) for the Baker's maps in section 7.1; the other parameters are set to 0. Sensitivities from $S3$ are shown in black at select parameter values.

map on the solid torus \mathbb{T}^2 is defined in cylindrical coordinates as,

$$(7.2) \quad \varphi_s([r, \theta, x^{(3)}]^T) = \begin{bmatrix} s_1 + (r - s_1)/4 + \cos \theta/2 \\ (2\theta + (s_2/4) \sin(4\theta)) \bmod (2\pi) \\ x^{(3)}/4 + \sin \theta/2 \end{bmatrix}.$$

The map can be expressed in Cartesian coordinates, denoted $[x^{(1)}, x^{(2)}, x^{(3)}]^T$, by left and right compositions of φ_s as in Eq. 7.2 with the following coordinate transformation and its inverse respectively: $x^{(1)} = r \cos \theta$, $x^{(2)} = r \sin \theta$. In Figure 6, we illustrate the effect of parameter variation on the Solenoid attractor, which is shown on the $x^{(1)}$ - $x^{(2)}$ plane. The subfigures show the points on an orbit of length 2 million at the corresponding values of s . On the left is the attractor of the unperturbed map at the standard value of $s = [1, 0]^T$. The center subfigure, at the value $s = [1, 1]^T$, shows a change in the *shape* of the attractor due to an s_2 perturbation, while the rightmost subfigure indicates a change in the *size* of the attractor due to an s_1 perturbation. Qualitatively, we can also note change in the distribution of points on the perturbed attractor. For instance, the effect of an increase in s_2 is to reduce the probability of visiting the outer rim of the attractor. Both these types of qualitative changes, i.e., in the position and shape of, and in the distribution on the attractor are indicative of changes in the SRB measure and are captured precisely by the computation of Ruelle's formula.

By inspecting Eq. 7.2, we can see that the r and $x^{(3)}$ coordinate directions are stable at

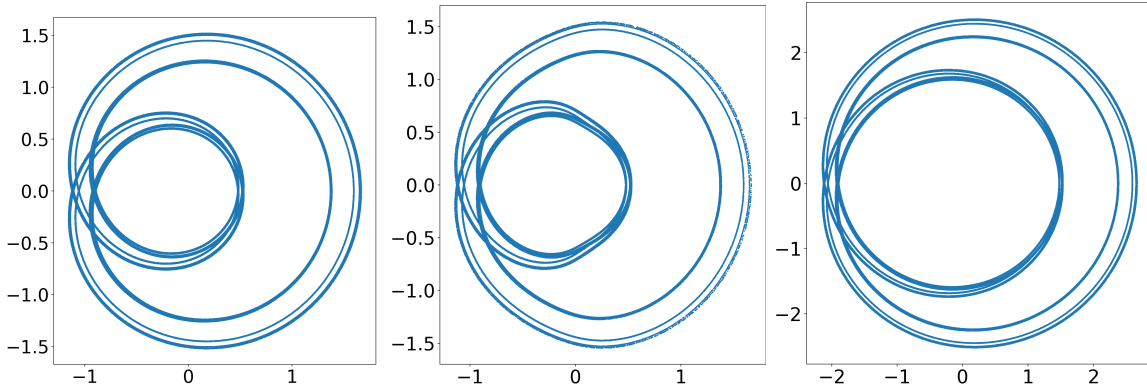


Figure 6. The projection of the Solenoid attractor on the $x^{(1)}$ - $x^{(2)}$ plane at $s = [1, 0]^T$ (left), $s = [1, 1]^T$ (center) and $s = [2, 0]^T$ (right) respectively.

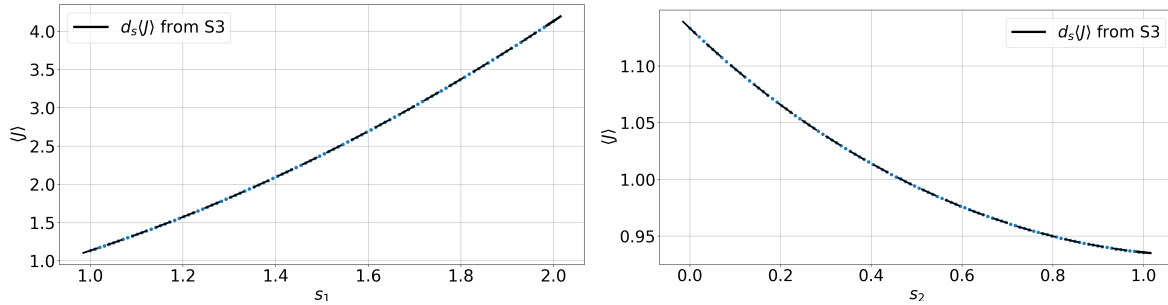


Figure 7. Linear response validation on the Solenoid attractor described in section 7.2. The sensitivities of $\langle J \rangle = \langle x^{(1)} \cdot x^{(1)} + x^{(2)} \cdot x^{(2)} \rangle$ with respect to the parameter s_1 (left) and s_2 (right) computed by S3 are shown as black lines at a number of parameter values on the $\langle J \rangle$ vs parameter curve. In each case, the other parameter is held constant at the reference value.

each phase point. The unstable direction, however, is not aligned with $\hat{\theta}$ everywhere. Thus, an s_1 perturbation corresponds to a stable vector field $\chi \in E^s$, and an s_2 perturbation has both stable and unstable components, albeit a small stable component.

As done in [17], had we split Ruelle's formula by decomposing the parameter perturbation into its stable and unstable components, the unstable contribution to the sensitivity is 0 for an s_1 perturbation. However, in the S3 algorithm, although the two terms of the split Ruelle's formula are called stable and unstable contributions, the perturbation vector field χ is not split along E^s and E^u . Hence, with S3, it is not a priori clear whether either contribution is zero in either type of parameter perturbation although we expect that for the s_1 perturbation, the stable contribution dominates, and for the s_2 , the unstable dominates.

7.2.1. Performance of S3. It is numerically verified that the S3 algorithm computes the correct sensitivity in both cases, as shown in Figure 7. The objective function, J is arbitrarily taken to be $J = r^2 = x^{(1)2} + x^{(2)2}$, and the sensitivity of $\langle J \rangle$ is computed at a range of values of s_1 (s_2) shown on the left (right) of Figure 7. The parameter that is not indicated on the horizontal axis is held constant at its reference value in each case. The computed

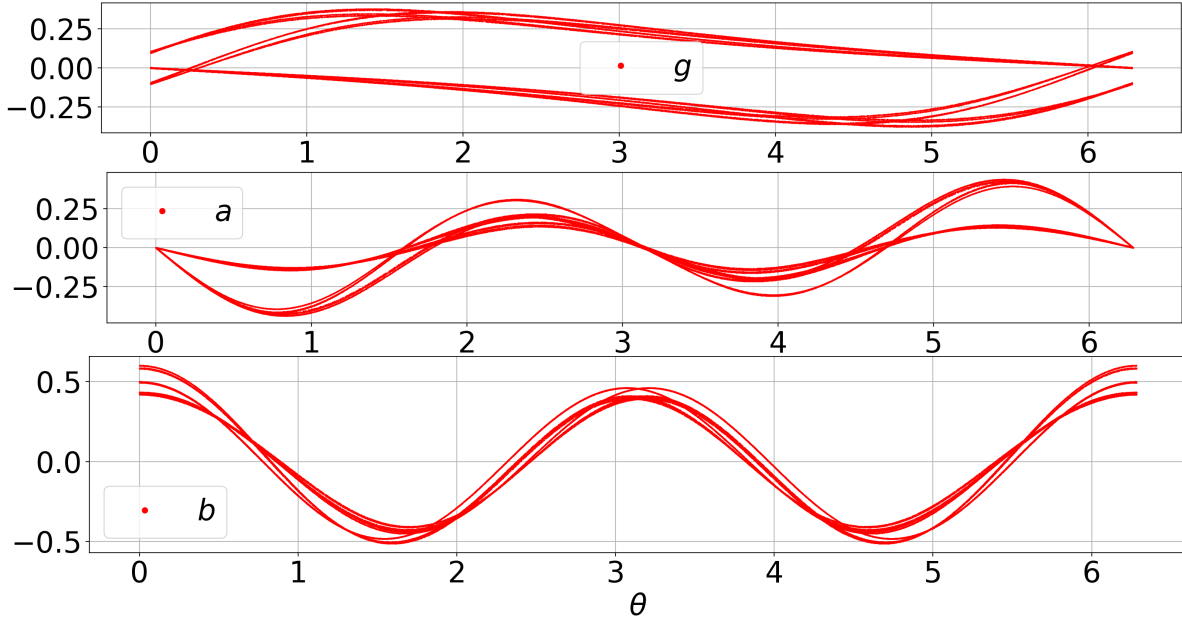


Figure 8. Three scalar fields computed for the unstable contribution: g (top), a (middle) and b (bottom), as a function of θ . These functions were computed by the S3 algorithm (section 4.1) using an orbit of length 100,000 of the Solenoid map (section 7.2) with $s = [1, 0]^T$.

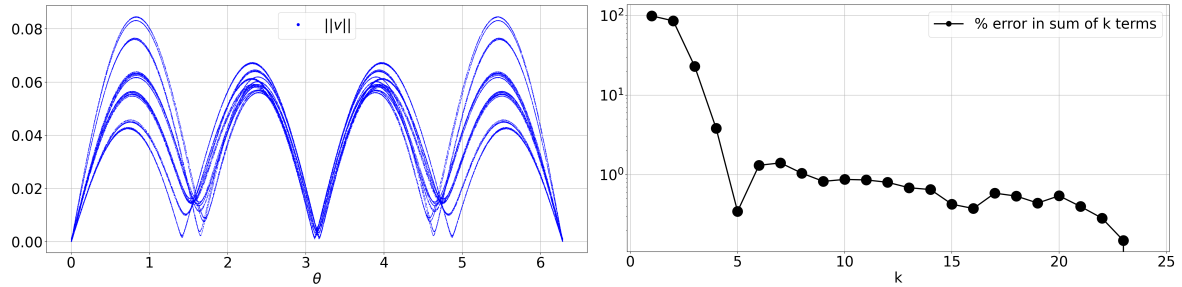


Figure 9. Left: the norm of the regularized tangent vector field computed by the S3 algorithm shown as a function of the θ coordinate. Right: percentage relative error in the unstable contribution when computed as a sum of the first k terms, as a function of k . The reference is taken as the unstable contribution computed with 24 terms. For both subfigures, the computations are performed along an orbit of length 100,000 of the Solenoid map (section 7.2) with $s = [1, 0]^T$.

S3 sensitivities closely match the slopes of the $\langle J \rangle$ -vs- s curves (shown as blue dots) that are computed from ergodic averages using orbits of length 160 million. The S3 sensitivities, which are linearly extrapolated and shown as black lines, are computed along orbits of length 3.2 million at each value of s . The source code to generate S3 results on the Solenoid map (as well as all other numerical results in this section) can be found at [13].

Having validated the S3 sensitivities on the Solenoid attractor, given the low dimensionality of this problem, we can further extract and visualize intermediate quantities computed

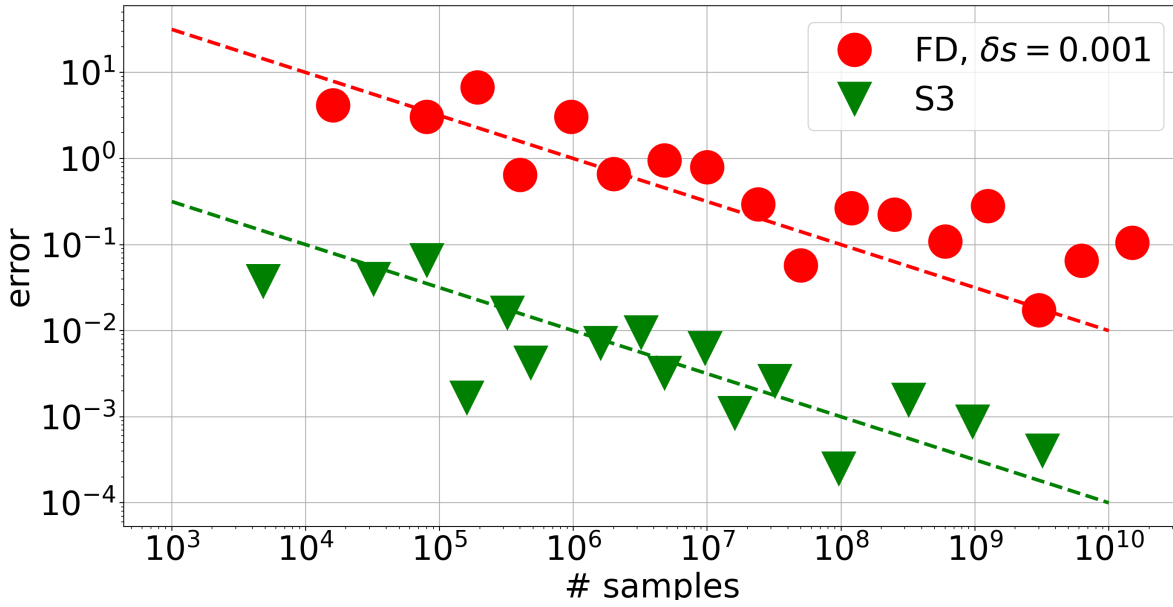


Figure 10. Comparison of relative error in the sensitivity of $\langle J \rangle$ to s_2 at $s = [1, 0]$ of the Solenoid map (section 7.2) as a function of the number of samples, between S3 and finite difference. The relative error is computed with respect to the true value, which is taken to be the S3 derivative obtained with $N = 9.6$ billion samples. The finite difference in the parameter s_2 used to calculate the derivatives is set to 0.001 in order to obtain the red dots. The green triangles are the derivatives computed using the S3 algorithm described in section 4.1. The dotted lines have a slope of -0.5.

by the S3 algorithm. To generate the remaining results of this section, s_1 is fixed at 1, and the derivative of $\langle J \rangle = \langle x^{(1)} \cdot x^{(1)} + x^{(2)} \cdot x^{(2)} \rangle$ with respect to s_2 is computed at $s = [1, 0]^T$.

One of our main results (Theorem 4.1) asserts the differentiability of the scalar field a and the vector field v in the unstable direction (see section 8 for the proof), and that g , a , b are Hölder continuous fields. Another main result (Theorem 4.3) proves the exponential convergence of the recursive computations of the functions v , a , b and g (see section 9 for the proof). While numerical verification of these analytically proved results is beyond the scope of this paper, we at least confirm the boundedness of the quantities a , b , g and $\|v\|$ on a long orbit. In Figure 8, we show the functions g , a and b computed by the S3 algorithm, which are associated with the unstable contribution. We plot the functions as a function of θ , which is close but not exactly parallel to the unstable direction at each point. Each subfigure shows the values of the corresponding functions at each point of an orbit of length 100,000 with $s = [1, 0]^T$. The S3 algorithm is run to compute the derivative $d_{s_2} \langle J \rangle$.

On the left hand side of Figure 9, we plot the norm of the regularized tangent vector field $\|v\|$ also as a function of the θ coordinate. Reassuringly, the norm of the regularized tangent vector field is always bounded. Further, as we noted in the previous subsection, the unstable contribution is the majority of the derivative in the case of the s_2 perturbation considered here. We confirm numerically that the unstable contribution dominates; the stable contribution is less than 0.01% of the overall sensitivity.

Figure 9 (right) provides numerical evidence for the rapid convergence (due to correlation decay) of Eq. 6.19 – the unstable contribution. We show the percentage relative error in the unstable contribution computed with the first k terms when compared to the baseline value calculated with 24 terms. Clearly, sums of terms in the series beyond 8 terms incur an error of less than 1% compared to the sum of the first 24 terms. In fact, each term for $k > 6$ evaluates to less than 1% of the overall sensitivity (calculated with 24 terms of the series).

In Figure 10, a comparison of the error convergence of S3 against a naïve finite difference calculation is shown using the Solenoid map. The finite difference approximation of the same linear response calculated with N samples is as follows,

$$(7.3) \quad \langle J, \partial_{s_2} \mu_s \rangle_{\text{FD}} = \frac{\langle J \rangle_N([s_1, s_2 + \delta s]) - \langle J \rangle_N([s_1, s_2 - \delta s])}{2\delta s},$$

where $\langle J \rangle_N(s)$ is an N -sample Monte Carlo estimate of $\langle J \rangle(s)$. Such an estimate can be computed either as an ergodic average along a single trajectory initialized Lebesgue almost everywhere, or as a sample average at samples according to μ on the attractor. To generate these plots efficiently, we do not compute ergodic averages along a single trajectory, as such a computation is a serial operation. Rather we sample average along multiple short trajectories in parallel, where each trajectory is initialized with a sample according to μ , which is achieved after a sufficiently long run-up time, starting from Lebesgue a.e. We observe in Figure 10 that the numerator of Eq. 7.3 is overwhelmed by statistical noise. As a result of the law of the iterated logarithm [25] that applies to $\langle J \rangle_N$ (asymptotically), the errors (ignoring the iterated logarithmic factor) in the finite difference decay as $\mathcal{O}(1/\sqrt{N})$. This is confirmed by the finite difference data points being well-approximated by a line with slope -0.5 (shown as a dotted red line). However, the central difference approximation grows as $\mathcal{O}(1/\delta s)$. As a result, the finite difference derivatives have much larger errors – in this case, two orders of magnitude larger errors – than the S3 derivatives (which are shown as green triangles), for the same number of samples. For instance, to achieve a 10% relative error, a central finite difference with $\delta s = 0.001$ requires more than a billion samples while the S3 algorithm shows less than 10% error even at 10,000 samples.

Note that the true value to compute relative error is taken to be the S3 derivative obtained from a ~ 10 billion sample computation, which is verified against the slope of the response curve $\langle J \rangle$ -vs- s_2 at $s_2 = 0$. Finally, we note that the error convergence in S3 is as predicted by the analysis in sections 8 and 9. In particular, in sections 9.1 and 9.2.2 respectively, we show that the error in the stable contribution and that in the unstable contribution diminish at the rate of $\mathcal{O}(\sqrt{\log \log N}/\sqrt{N})$, with N samples. Consistent with these results, the dotted green line, which has a slope equal to -0.5, well approximates the S3 data points in Figure 10 (we may ignore the $\sqrt{\log \log N}$ factor, which only has a negligible effect on the slope).

8. Proof of Theorem 4.1. In this section, we prove Theorem 4.1, which establishes that the S3 decomposition of Ruelle’s formula into stable and unstable contributions (Eq. 4.3) is well-defined. We show that the S3 decomposition exists and is differentiable on the unstable manifold. In particular, we prove that the regularized perturbation field, v , that is the limit of the sequence $\{v^n\}$ in Eq. 4.1, exists. This proves Theorem 4.1-1. The second statement, Theorem 4.1-2., is shown by proving that this vector field v is differentiable on the unstable

manifold. We then prove that the differentiability in the unstable direction of v implies that of the scalar field a , and hence Theorem 4.1-2. is proved. First we start by proving the existence and uniqueness of v . Before we begin, we establish some notation for oblique projection operators on vector fields, and describe their properties that we use in the proofs.

Notation 8.1. Let $\mathcal{S}_x : T_x M \rightarrow T_x M$ denote the linear operator that gives the component of a tangent vector in E_x^s , in a direct sum of components along E_x^u and E_x^s . If $v_x = v_x^u + v_x^s$ where $v_x^u \in E_x^u$ and $v_x^s \in E_x^s$, then, $\mathcal{S}_x v_x := v_x^s$. Applying \mathcal{S}_x to every point on M would result in a linear operator on vector fields of M , hereafter denoted \mathcal{S} .

Remark 8.2. Note that \mathcal{P}_x is an orthogonal projector. Its norm is therefore 1. In contrast, the operator \mathcal{S}_x is not an orthogonal projector; \mathcal{S}_x is uniformly bounded over M , i.e., $S := \sup_{x \in M} \|\mathcal{S}_x\|$ is finite.

Remark 8.3. It follows from their definition that both operators are idempotent, i.e., $\mathcal{P}^2 = \mathcal{P}$ and $\mathcal{S}^2 = \mathcal{S}$.

Remark 8.4. Due to the covariance of E^s and E^u , i.e., $d\varphi_x^n E_x^s = E_{\varphi^{n,x}}^s$ and $d\varphi_x^n E_x^u = E_{\varphi^{n,x}}^u$, the operator \mathcal{S} satisfies $d\varphi_x^n \mathcal{S}_x = \mathcal{S}_{\varphi^{n,x}} d\varphi_x^n$. Operating on vector fields on M , this equality leads to $d\varphi^n \mathcal{S} = \mathcal{S} d\varphi^n$.

Remark 8.5. At every $x \in M$, both \mathcal{S}_x and \mathcal{P}_x map E_x^u to 0 by their definitions. Also by definition, for any $v_x \in T_x M$, both $v_x - \mathcal{S}_x v_x$ and $v_x - \mathcal{P}_x v_x$ are in E_x^u . We thus have $\mathcal{P}_x v_x = \mathcal{P}_x \mathcal{S}_x v_x$ and $\mathcal{S}_x v_x = \mathcal{S}_x \mathcal{P}_x v_x$. The equivalent expressions, as operators on vector fields, are $\mathcal{P} \mathcal{S} = \mathcal{P}$ and $\mathcal{S} \mathcal{P} = \mathcal{S}$.

We now prove that a regularized perturbation field v exists, which is the limit of the tangent equation solved with repeated projections (section 5.2). We note that, in all the proofs that follow, the constants C and λ refer to the eponymous constants in the definition of uniform hyperbolicity (section 3), and the constant S refers to the norm of the stable projection operator \mathcal{S} , as defined above (Remark 8.2); all other constants, such as A, c , etc. may vary from line to line.

8.1. Existence and uniqueness of a regularized perturbation field.

Lemma 8.6. For any bounded vector field $\chi : M \rightarrow \mathbb{R}^m$, there exists a unique bounded vector field v on M that satisfies

$$(8.1) \quad v = \mathcal{P}(d\varphi v + \chi)$$

Note that because $\mathcal{P}^2 = \mathcal{P}$, Eq. 8.1 implies that $\mathcal{P}v = v$. In other words, at every $x \in M$, v_x is orthogonal to the one-dimensional unstable subspace E_x^u . Also, a vector field χ being bounded means that $\sup_{x \in M} \|\chi_x\|$ is finite.

Proof. We first prove existence. Let $v^0 = 0$ be an arbitrary bounded vector field on M . Let $v^{k+1} = \mathcal{P}(d\varphi v^k + \chi)$ for $k = 0, 1, \dots$. We will show that for each $x \in M$, $\{v_x^k, k = 0, 1, \dots\}$ is a Cauchy sequence and thus converges to a limit, namely v_x .

From the definition of v^k and the linearity of the operators involved, we have $v^{k+1} - v^k = \mathcal{P} d\varphi(v^k - v^{k-1}) = (\mathcal{P} d\varphi)^k(v^1 - v^0)$. Here, we can use the relations between \mathcal{P}, \mathcal{S} , and $d\varphi$ (See Remarks 8.4 and 8.5) to simplify the linear operator as follows. Since $\mathcal{P} = \mathcal{P}\mathcal{S}$,

$(\mathcal{P} d\varphi)^k = (\mathcal{P} \mathcal{S} d\varphi)^k = (\mathcal{P} d\varphi \mathcal{S})^k$, where the second equality follows from Remark 8.4. Now using $\mathcal{S}\mathcal{P} = \mathcal{S}$ (Remark 8.5), $(\mathcal{P} d\varphi)^k = (\mathcal{P} d\varphi \mathcal{S})^k = \mathcal{P} d\varphi (d\varphi \mathcal{S})^{k-1}$, and finally using Remark 8.4, $(\mathcal{P} d\varphi)^k = \mathcal{P} d\varphi (d\varphi \mathcal{S})^{k-1} = \mathcal{P} d\varphi^k \mathcal{S}$.

From inequality 3.4 and the uniform boundedness of $\|\mathcal{S}_x\|$ by S (Remark 8.2), $\|d\varphi_x^k \mathcal{S}_x\| \leq C \lambda^k S$. Together with $\|\mathcal{P}_x\| = 1$, we have a uniform bound

$$(8.2) \quad \|(\mathcal{P} d\varphi)_x^k\| = \|\mathcal{P}_{\varphi^{kx}} d\varphi_x^k \mathcal{S}_x\| \leq C \lambda^k S, \quad \forall x \in M.$$

Thus,

$$(8.3) \quad \|v_x^{k+1} - v_x^k\| = \|(\mathcal{P} d\varphi)_{\varphi^{-kx}}^k (v_{\varphi^{-kx}}^1 - v_{\varphi^{-kx}}^0)\| \leq C \lambda^k S \|v_{\varphi^{-kx}}^1 - v_{\varphi^{-kx}}^0\|.$$

Because v^0 is bounded by definition, and v^1 is bounded due to the boundedness of v^0, χ , and $d\varphi$, there exists an $A > 0$ such that $C S \|v_x^1 - v_x^0\| < A$ for all $x \in M$. Thus, for all $k \geq 0$, and $x \in M$,

$$(8.4) \quad \|v_x^{k+1} - v_x^k\| \leq A \lambda^k.$$

And, for all $m > n \geq 0$,

$$(8.5) \quad \|v_x^m - v_x^n\| \leq \sum_{k=n}^{m-1} \|v_x^{k+1} - v_x^k\| \leq A \sum_{k=n}^{m-1} \lambda^k < A \frac{\lambda^n}{1-\lambda}.$$

Then, given $\epsilon > 0$, choosing $N > \lceil \log |A/(\epsilon(1-\lambda))| / \log |1/\lambda| \rceil$, for all such that $m > n \geq N$,

$$(8.6) \quad \|v_x^m - v_x^n\| \leq \epsilon, \quad \forall x \in M.$$

Thus $\{v_x^n\}$ is a *uniform* Cauchy sequence, and thus the sequence $\{v^n\}$ converges uniformly on M .

Equation 8.5, applied to $n = 0$, also implies that $\|v_x^m\| \leq \|v_x^0\| + \frac{A}{1-\lambda}$, for all x and m . The limit of the Cauchy sequence thus uniformly satisfies the same bound.

We now show this limit, defined by the vector field v as $v_x := \lim_{n \rightarrow \infty} v_x^n$, is **unique** in satisfying Eq. 8.1. Suppose Δv is a bounded vector field such that $v + \Delta v$ also satisfies Eq. 8.1. Without loss of generality, let Δv be bounded by 1, i.e., $\|\Delta v_x\| \leq 1$ for all $x \in M$. Due to the linearity of the operators involved, $\Delta v = \mathcal{P} d\varphi \Delta v$, and by iteration, $\Delta v = (\mathcal{P} d\varphi)^k \Delta v$ for any $k \in \mathbb{N}$. Using Eq. 8.2, $\|(\Delta v)_x\| \leq C \lambda^k S \|(\Delta v)_{\varphi^{-kx}}\| \leq C \lambda^k S$ for all $x \in M$. Because $\lambda < 1$ and this inequality holds for all k , $\|\Delta v_x\|$ must be 0. Thus $\Delta v = 0$. The uniqueness of v follows. ■

We remark that, without loss of generality, starting from $v^0 = 0$, we obtain the following simple expressions for the regularized tangent vector field v ,

$$(8.7) \quad v = \sum_{n=0}^{\infty} (\mathcal{P} d\varphi)^n \mathcal{P} \chi = \sum_{n=0}^{\infty} \mathcal{P} d\varphi^n \mathcal{S} \mathcal{P} \chi = \sum_{n=0}^{\infty} \mathcal{P} d\varphi^n \mathcal{S} \chi,$$

where we have used Remark 8.5 to obtain the third equality. This establishes the existence of the regularized perturbation field v , and completes the proof of Theorem 4.1-1. Having

shown that v exists, we now show that it is differentiable in the unstable direction. This differentiability is used to prove Theorem 4.1-2. Before this, we first show that q is differentiable in its own direction. Although it is known that self-derivatives of the unstable/stable subspaces exist (see, for instance, Remark after Lemma 19.1.7 of [35]), we include a proof here for completion.

8.2. Existence of self-derivative of the unstable direction. We refer to as the unstable self-derivative, the vector field $w := d_\xi^2 \Phi^x$. We now show its existence.

Lemma 8.7. *There exists a unique, bounded vector field w that satisfies*

$$(8.8) \quad w = \mathcal{P} \frac{d^2 \varphi(q, q) + d\varphi w}{\alpha^2},$$

where $\alpha := \|d\varphi q\|$.

Note that, since $w = \mathcal{P}w$, w is orthogonal to q .

Proof. Consider a sequence of vector fields $\{w^n\}$ that satisfies the recurrence relation

$$(8.9) \quad w^{n+1} = \mathcal{P} \frac{d^2 \varphi(q, q) + d\varphi w^n}{\alpha^2}$$

We will now show that w^n is a uniformly Cauchy sequence and hence converges uniformly. From the above recurrence relation,

$$(8.10) \quad w^{n+1} - w^n = \frac{1}{\alpha^2} \mathcal{P} d\varphi (w^n - w^{n-1}),$$

iterating which, gives, for all $n \in \mathbb{N}$

$$(8.11) \quad w^{n+1} - w^n = \frac{1}{\prod_{k=0}^{n-1} \alpha_{\varphi^{-k}}^2} (\mathcal{P} d\varphi)^n (w^1 - w^0).$$

Then, using i) $(\mathcal{P} d\varphi)^n = \mathcal{P} d\varphi^n \mathcal{S}$, which is shown in Lemma 8.6, and ii) $\|\mathcal{P}_x\| = 1$, at all $x \in M$,

$$(8.12) \quad \|w_x^{n+1} - w_x^n\| \leq \frac{1}{\prod_{k=0}^{n-1} \alpha_{\varphi^{-k}x}^2} \|d\varphi_{\varphi^{-n}x}^n \mathcal{S}_{\varphi^{-n}x} (w_{\varphi^{-n}x}^1 - w_{\varphi^{-n}x}^0)\|.$$

Now using i) $\prod_{k=0}^{n-1} \alpha_{\varphi^{-k}x} \geq (1/C)\lambda^{-n}$, and ii) $\|d\varphi_x^n \mathcal{S}_x\| \leq C\lambda^n S$, for all $x \in M$, both of which follow from the definition of uniform hyperbolicity,

$$(8.13) \quad \|w_x^{n+1} - w_x^n\| \leq C^3 \lambda^{3n} S \|w_{\varphi^{-n}x}^1 - w_{\varphi^{-n}x}^0\|.$$

Clearly, since the map from w^0 to w^1 is bounded, and by assumption w^0 is bounded, there exists a constant A such that $A := \sup_{x \in M} \|w_x^1 - w_x^0\|$. Hence, for any $m > n \geq 0$,

$$(8.14) \quad \|w_x^m - w_x^n\| \leq A S C^3 \sum_{k=n}^{m-1} \lambda^{3k} \leq A S C^3 \frac{\lambda^{3n}}{1 - \lambda^3}.$$

Since the above inequality holds for all x , the sequence w_x^n is uniformly Cauchy and hence converges uniformly. Let $w := \lim_{n \rightarrow \infty} w^n$. To show that w is unique, suppose w^n and \tilde{w}^n are two different sequences that both satisfy Eq. 8.9. Then, at every $x \in M$,

$$(8.15) \quad \|w_x^n - \tilde{w}_x^n\| \leq \frac{1}{\alpha_x^2} \|d\varphi_{\varphi^{-1}x} \mathcal{S}_{\varphi^{-1}x} (w_{\varphi^{-1}x}^{n-1} - \tilde{w}_{\varphi^{-1}x}^{n-1})\|$$

$$(8.16) \quad \leq A' \lambda^{3n},$$

where the second inequality is obtained by recursively applying the first n times and then applying the definition of uniform hyperbolicity as done previously. Taking the limit $n \rightarrow \infty$ on both sides, we obtain that at every $x \in M$, $\|w_x - \tilde{w}_x\| = 0$. Thus, w is a unique vector field independent of w^0 . \blacksquare

We note that the vector field w that satisfies Eq. 8.8 is also $\partial_\xi q$. This relationship can be derived by differentiating with respect to ξ the following equation that expresses the definition of the unstable CLV, q :

$$(8.17) \quad \alpha_{\varphi x} q_{\varphi x} = d\varphi_x q_x.$$

We derive this relationship in detail in section 6.1. As described in section 6, the practical computation of the vector field w involves repeated application of Eq. 8.9, by choosing, without loss of generality, $w_x^0 = 0$, at all x . Choosing an initial phase point x sampled according to μ , one then obtains the values $w_{\varphi^n x}^n$ along the orbit of x . As n increases, these values exponentially approach the true value of w along that orbit, as the proof of Lemma 8.7 shows. The convergence of the numerical procedure to compute w , which we have shown here, is needed to prove the convergence of the method (in the S3 algorithm, section 4.1) to compute the unstable derivative of v . We focus on this convergence next, which ultimately establishes the differentiability of the S3 decomposition.

8.3. Convergence of the unstable projections of the regularized tangent solutions.

The S3 decomposition of the perturbation field χ into $a q$ and $\chi - a q$ is differentiable on the unstable manifolds, if $y := \partial_\xi v$ exists. To see why, we first note that the scalar field a is the limit of the iterative projections of the sequence v^n , which in practice is obtained by solving the regularized tangent equation (Eq. 5.1). We formally establish the existence of a by showing that the iterative procedure used to obtain it converges.

Lemma 8.8. *Let $\{a^n\}$, $n \in \mathbb{Z}^+$, be a sequence of scalar fields determined by a sequence of vector fields, $\{v^n\}$, that satisfies i) $v_x^n \cdot q_x = 0$, $\forall x \in M$, $n \in \mathbb{Z}^+$, and,*

$$(8.18) \quad \text{ii) } v^{n+1} = (d\varphi) v^n + \chi - a^{n+1} q, \quad n \in \mathbb{Z}^+.$$

Then, $\{a^n\}$ converges uniformly.

Note that i) and ii) above constitute the iterative procedure to compute the regularized tangent solution in the S3 algorithm (section 4.1). The sequence $\{v^n\}$ is identical to the sequence defined in Lemma 8.6.

Proof. The scalar fields a^{n+1} are the projections of $d\varphi v^n + \chi$ on q ,

$$(8.19) \quad a^{n+1} = q^T (d\varphi v^n + \chi).$$

As shown in Lemma 8.6, the sequence v^n converges uniformly. Hence, also using the fact that $\varphi \in \mathcal{C}^2(M)$, for every $\epsilon > 0$, there exists an $N \in \mathbb{N}$ such that for all $m, n \geq N$,

$$(8.20) \quad \|v_x^m - v_x^n\| < \frac{\epsilon}{\sup_{x \in M} \|d\varphi_x\|}, \quad \forall x \in M.$$

Hence, for all $m, n \geq N$, and for all $x \in M$,

$$(8.21) \quad \begin{aligned} |a_x^{m+1} - a_x^{n+1}| &\leq \|q_x\| \|d\varphi_x\| \|v_x^m - v_x^n\| \\ &\leq \left(\sup_{x \in M} \|d\varphi_x\| \right) \|v_x^m - v_x^n\| \leq \epsilon. \end{aligned}$$

Thus, $\{a^n\}$ converges uniformly. ■

We define the limit of the sequence $\{a^n\}$ by taking the limit as $n \rightarrow \infty$ of Eq. 8.19,

$$(8.22) \quad a := \lim_{n \rightarrow \infty} a^n = q^T(d\varphi v + \chi),$$

where $v := \lim_{n \rightarrow \infty} v^n$ is as defined in Lemma 8.6. In other words, we have the following relationship between a and v ,

$$(8.23) \quad \chi - aq = v - d\varphi v.$$

As we have shown in Lemma 8.6, the limit v is a unique vector field, independent of the initial condition for the iteration (Eq. 5.1 or equivalently, Eq. 8.18) provided that v^0 is bounded.

8.4. Route to showing existence and differentiability of the S3 decomposition. So far, we have shown that a bounded vector field v exists that is orthogonal to the unstable manifold, and the asymptotic solution of a regularized tangent equation (Eq. 5.1). We showed the existence of the stable contribution by proving that the scalar field a , which represents the component in the unstable direction in decomposing χ , is related to v (Eq. 8.23). Further, we established that a is achieved in the same iterative procedure used for v .

In order to complete the proof of Theorem 4.1, we must show that the S3 decomposition of χ is differentiable on the unstable manifold. That is, we must show that the scalar field a is differentiable on the unstable manifold. Lemma 8.7 is a result toward this purpose. Using Eq. 8.23, we can see that if v , and hence $d\varphi v$ are differentiable with respect to ξ , and since χ is differentiable, by assumption, in all directions, we can then conclude that aq is differentiable in the unstable direction by Eq. 8.23.

Further, by Lemma 8.7, the derivative $w := \partial_\xi q$ exists. Thus, the scalar field a is differentiable on the unstable manifold, if v is. Therefore, it remains to show the existence of $\partial_\xi v$, in order to complete the proof of Theorem 4.1-1 and 2.

8.5. Differentiability of v in the unstable direction.

Proposition 8.9. *The regularized perturbation field v is differentiable on the unstable manifold, i.e., $\partial_\xi v$ exists.*

We prove this proposition using the following lemma.

Lemma 8.10. *Let $\{\zeta^n\}$ be a uniformly exponentially converging sequence of vector fields. That is, $\{\zeta^n\}$ is uniformly converging such that there exists an $A > 0$ for which $\|\zeta_x^{n+1} - \zeta_x^n\| \leq A \lambda^n$, for all $x \in M$, and $n \in \mathbb{Z}^+$. Given a bounded vector field y^0 , the sequence $\{y^n\}$ that satisfies the following recurrence,*

$$(8.24) \quad y^{n+1} = \frac{1}{\alpha} \mathcal{P} d\varphi y^n + \zeta^{n+1}, \quad \forall n \in \mathbb{Z}^+,$$

converges uniformly to a unique vector field, $y := \lim_{n \rightarrow \infty} y^n$.

Proof. Using the recurrence relation, for all $n \in \mathbb{N}$,

$$(8.25) \quad y^{n+1} - y^n = \frac{1}{\alpha} \mathcal{P} d\varphi (y^n - y^{n-1}) + (\zeta^{n+1} - \zeta^n).$$

Applying this equation iteratively,

$$(8.26) \quad y^{n+1} - y^n = \frac{1}{\prod_{k=0}^{n-1} \alpha \circ \varphi^{-k}} (\mathcal{P} d\varphi)^n (y^1 - y^0)$$

$$(8.27) \quad + \sum_{k=0}^{n-1} \frac{1}{\prod_{j=0}^{k-1} \alpha \circ \varphi^{-j}} (\mathcal{P} d\varphi)^k (\zeta^{n-k+1} - \zeta^{n-k}).$$

Using i) the relation $(\mathcal{P} d\varphi)^n = \mathcal{P} d\varphi^n \mathcal{S}$ – which is derived in Lemma 8.6 using Remarks 8.4 and 8.5 –, ii) $\|\mathcal{P}_x\| = 1$, and iii) $\prod_{k=0}^{n-1} \alpha_{\varphi^{-k}x} \geq (1/C)\lambda^{-n}$ at any $x \in M$,

$$(8.28) \quad \begin{aligned} \|y_x^{n+1} - y_x^n\| &\leq C^2 \lambda^{2n} S \|y_{\varphi^{-n}x}^1 - y_{\varphi^{-n}x}^0\| \\ &+ C^2 S \sum_{k=0}^{n-1} \lambda^{2k} \|\zeta_{\varphi^{-k}x}^{n-k+1} - \zeta_{\varphi^{-k}x}^{n-k}\|. \end{aligned}$$

Now since $\{\zeta^n\}$ is uniformly exponentially converging,

$$(8.29) \quad \|\zeta_{\varphi^{-k}x}^{n-k+1} - \zeta_{\varphi^{-k}x}^{n-k}\| \leq A \lambda^{n-k}.$$

Further, since y^0, ζ^1 are bounded vector fields, and $\mathcal{P} d\varphi$ is bounded, y^1 is a bounded vector field. Hence, there exists some constant A_1 such that for any $x \in M$,

$$(8.30) \quad \|y_{\varphi^{-n}x}^1 - y_{\varphi^{-n}x}^0\| < A_1.$$

Using both the above relationships ((8.29) and (8.30)) in (8.28),

$$\|y_x^{n+1} - y_x^n\| \leq C^2 \lambda^{2n} S A_1 + A C^2 S \lambda^n / (1 - \lambda) \leq A_2 \lambda^n.$$

Hence, for $m \geq n > 0$, and all $x \in M$,

$$(8.31) \quad \|y_x^m - y_x^n\| \leq \sum_{k=n}^{m-1} A_2 \lambda^k < A_2 \frac{\lambda^n}{1 - \lambda}.$$

Thus, $\{y^n\}$ is uniformly Cauchy and converges uniformly.

To see that the limit $y := \lim_{n \rightarrow \infty} y^n$ is unique, let y^n and \tilde{y}^n be two different bounded sequences that satisfy Eq. 8.24, and converge to y and \tilde{y} respectively. Then,

$$(8.32) \quad y^n - \tilde{y}^n = \frac{1}{\alpha} \mathcal{P} d\varphi (y^{n-1} - \tilde{y}^{n-1}),$$

which can be applied recursively to yield,

$$(8.33) \quad y^n - \tilde{y}^n = \frac{1}{\prod_{k=0}^{n-1} \alpha \circ \varphi^{-k}} (\mathcal{P} d\varphi)^n (y^0 - \tilde{y}^0) = \frac{1}{\prod_{k=0}^{n-1} \alpha \circ \varphi^{-k}} \mathcal{P} d\varphi^n \mathcal{S}(y^0 - \tilde{y}^0).$$

Since both y^0 and \tilde{y}^0 are bounded, the operator norm of \mathcal{S}_x is uniformly bounded above, and from the definition of uniform hyperbolicity, there exists some $c > 0$ such that for all n , and all $x \in M$, we have

$$(8.34) \quad \|\tilde{y}_x^n - y_x^n\| \leq c \lambda^{2n}.$$

Thus, $\lim_{n \rightarrow \infty} (\tilde{y}_x^n - y_x^n) = 0 \in \mathbb{R}^m$ for every $x \in M$. Hence, the limit y is unique.

Now we prove Proposition 8.9. We set

$$(8.35) \quad \zeta^{n+1} = \mathcal{P} \left(\frac{d^2\varphi(q, v^n)}{\alpha} + d\chi q \right) + (\partial_\xi \mathcal{P})(d\varphi v^n + \chi),$$

where the sequence $\{v^n\}$ is as defined in Lemma 8.6; $d^2\varphi_x(\cdot, \cdot) : T_x M \times T_x M \rightarrow T_{\varphi x} M$ is a bilinear form representing the second-order derivative of φ at $x \in M$. In order to apply Lemma 8.10, we must show that $\{\zeta^n\}$ is a bounded, uniformly exponentially converging sequence. First we note that the projection operator \mathcal{P} is differentiable in the unstable direction. Using the matrix representation of \mathcal{P} , and Lemma 8.7, its derivative is given by

$$(8.36) \quad \partial_\xi \mathcal{P} = -\partial_\xi (qq^T) = -(wq^T + qw^T),$$

from which we see that the operator norm of $\partial_\xi \mathcal{P}$ is bounded on M . Because $d\varphi \in C^2(M)$ by assumption, $\|d\varphi_x\|$ and $\|d^2\varphi_x\|$ are also bounded on M ; χ and $d\chi$ are bounded by assumption. Now, the sequence $\{v^n\}$ is uniformly bounded on M and \mathbb{Z}^+ ($\because \{v^n\}$ is bounded and uniformly convergent, by Lemma 8.6). Thus, $\{\zeta^n\}$ defined in Eq. 8.35 is a uniformly bounded sequence.

Now to show that $\{\zeta^n\}$ is uniformly exponentially converging, we use its definition, Eq. 8.35, to get

$$(8.37) \quad \zeta^{n+1} - \zeta^n = \partial_\xi \mathcal{P} d\varphi (v^{n+1} - v^n) + \frac{\mathcal{P}}{\alpha} d^2\varphi (q, (v^{n+1} - v^n)).$$

Since $\partial_\xi \mathcal{P}$, $d\varphi$ and $d^2\varphi$ are bounded and $\|\mathcal{P}\| = 1$, and using Eq. 8.3, there exists some $c > 0$ such that, for all $x \in M$,

$$(8.38) \quad \|\zeta_x^{n+1} - \zeta_x^n\| \leq \left(\|(\partial_\xi \mathcal{P})_x\| \|d\varphi_{\varphi^{-1}x}\| + \frac{\|d^2\varphi_x(q_x, \cdot)\|}{\alpha} \right) A \lambda^n := c \lambda^n.$$

Thus, using the same argument following Eq. 8.3 in Lemma 8.6, we can show that $\{\zeta^n\}$ converges uniformly. Further, the limit $\zeta := \lim_{n \rightarrow \infty} \zeta^n$ is unique, and defined by taking the limit of Eq. 8.35,

$$(8.39) \quad \zeta = \mathcal{P}\left(\frac{d^2\varphi(q, v)}{\alpha} + d\chi \cdot q\right) + (\partial_\xi \mathcal{P})(d\varphi v + \chi),$$

Therefore, $\{\zeta^n\}$, as defined in Eq. 8.35, is a uniformly bounded, uniformly exponentially converging sequence of vector fields. Now applying Lemma 8.10, there exists a unique, bounded vector field y that satisfies

$$(8.40) \quad y = \frac{\mathcal{P} d\varphi y}{\alpha} + \zeta.$$

Differentiating with respect to ξ the constraint, Eq. 8.1, which is satisfied by the regularized perturbation field v , we see that if the derivative $\partial_\xi v$ exists, it must satisfy Eq. 8.40 (replacing y), with ζ defined in Eq. 8.39. Since a vector field y that satisfies Eq. 8.40 exists and is unique (Lemma 8.10), the regularized perturbation field v is indeed differentiable. This completes the proof of Proposition 8.9. Further, the computation of its derivative, using the sequence of vector fields $\{y^n\}$ used in the proof of Lemma 8.10, converges exponentially along almost every trajectory. Note that the evaluation of y along a trajectory, with ζ defined in Eq. 8.39, is precisely that derived in section 6.3.

Recall the argument (section 8.4) that the differentiability (with respect to ξ) of v implies that of a . This completes the proof of Theorem 4.1-2., and hence the first two parts of Theorem 4.1. To complete the proof of Theorem 4.1-3, we provide a constructive proof of the unstable derivative $b = \partial_\xi a$. In a similar vein to Lemmas 8.6, 8.7 and 8.10, this proof shows that a trajectory-based computation adopted in S3 converges exponentially, in this case, to the true values of b .

8.6. Convergence of the derivative of $\{a^n\}$. We now show that the iterative algorithm for the scalar derivative $b^n := \partial_\xi a^n$ converges uniformly. Expanding Eq. 8.35 to make the appearance of $b^n := \partial_\xi a^n$ explicit, by using the definition of a^n (Lemma 8.8),

$$y^{n+1} = \frac{d\varphi y^n}{\alpha} + \frac{d^2\varphi(v^n, q)}{\alpha} + d\chi q - a^{n+1}w - b^{n+1}q.$$

Taking inner product with q and using $w_x \cdot q_x = 0$ at all $x \in M$ (Lemma 8.7),

$$(8.41) \quad b^{n+1} = \left(\frac{d\varphi y^n}{\alpha} - y^{n+1} + \frac{d^2\varphi(v^n, q)}{\alpha} + d\chi q \right) \cdot q.$$

Lemma 8.11. *The sequence $\{b^n\}$ defined in Eq. 8.41 converges uniformly where i) the sequence $\{y^n\}$ satisfies Eq. 8.24, and, ii) $\{v^n\}$ satisfies Eq. 5.2.*

Proof. We prove that the sequence of vector fields $\{\tau^n\}$ given by

$$(8.42) \quad \tau^{n+1} = \frac{d\varphi y^n}{\alpha} - y^{n+1} + \frac{d^2\varphi(v^n, q)}{\alpha} + d\chi q.$$

converges uniformly. From the above definition, and using the linearity of $d^2\varphi(\cdot, q)$, at any $x \in M$, and all $n > m \geq 0$,

$$(8.43) \quad \|\tau_x^{n+1} - \tau_x^{m+1}\| \leq \frac{\|d\varphi_x\|}{\alpha_x} \|y_x^n - y_x^m\| + \|y_x^{n+1} - y_x^{m+1}\| + \frac{\|d^2\varphi_x(v_x^n - v_x^m, q_x)\|}{\alpha_x}.$$

Recall that $\varphi \in C^3(M)$ and hence $\|d\varphi_x\|$ and $\|d^2\varphi_x(\cdot, \cdot)\|$ are both uniformly bounded; from uniform hyperbolicity, $1/\alpha_x \leq C\lambda$, at all $x \in M$. Let $\epsilon > 0$ be given. Using Lemma 8.10, there exists an $N_y \in \mathbb{N}$ such that for all $x \in M$ and $m, n \geq N_y$, $\|y_x^n - y_x^m\| < \epsilon/(3C\lambda \sup_{x \in M} \|d\varphi_x\|)$. Similarly, using Lemma 8.6, there exists an $N_y \in \mathbb{N}$ such that for all $x \in M$ and $m, n \geq N_y$, $\|v_x^n - v_x^m\| < \epsilon/(3C\lambda \sup_{x \in M} \|d^2\varphi_x(q, \cdot)\|)$. Choosing $N = \max\{N_y, N_y\}$, for all $m, n \geq N$, and all $x \in M$, $\|\tau_x^n - \tau_x^m\| \leq \epsilon$. Thus, $\{\tau^n\}$ converges uniformly. Since at all $x \in M$, $b_x^n = \tau_x^n \cdot q_x$, the sequence $\{b^n\}$ also converges uniformly. Moreover, note from (8.43) that the speed of convergence is exponential, since both $\{v^n\}$ and $\{y^n\}$ are exponentially uniformly converging as shown in Lemmas 8.6 and 8.10 respectively. The limit is unique since,

$$(8.44) \quad b := \lim_{n \rightarrow \infty} b^n = \left(\lim_{n \rightarrow \infty} \tau^n \right) \cdot q = \left(d\chi q - y + \frac{d\varphi y + d^2\varphi(v, q)}{\alpha} \right) \cdot q. \quad \blacksquare$$

9. Proof of Theorem 4.3. In this section, we complete the proof of Theorem 4.3, which establishes the convergence of the S3 algorithm (section 4.1). In particular, we prove that the ergodic averages we compute in the S3 algorithm (section 4.1) for the stable and unstable contributions converge to their true values.

9.1. Convergence of the stable contribution. Having shown the S3 decomposition is differentiable on the unstable manifold (section 8), we now derive an alternative expression for the stable contribution. This expression leads to a direct computation of the stable contribution using the regularized tangent equation (section 5.2). We then show that this computation converges to the true stable contribution.

Proposition 9.1. *The error in the numerically computed stable contribution converges as $\mathcal{O}(\sqrt{\log \log N}/\sqrt{N})$, where N is the trajectory length used in the computation.*

Proof. Taking $\lim_{m \rightarrow \infty}$ of Eq. 8.5, $\|v_x^n - v_x\| < A \frac{\lambda^n}{1 - \lambda}$, $\forall x \in M$, $n \in \mathbb{Z}^+$. Hence, $\{v^n\}$ is a uniformly bounded sequence. Since dJ is bounded by assumption, by Lebesgue dominated convergence on the sequence of functions $\{dJ \cdot v^n\}$, $\lim_{n \rightarrow \infty} \langle dJ \cdot v^n, \mu \rangle = \langle dJ \cdot v, \mu \rangle$. From Lemma 8.6, an explicit expression for v^n starting from $v^0 = 0 \in \mathbb{R}^m$ is $v^n = \sum_{k=0}^{n-1} d\varphi^k(\chi - a^{n-k}q)$. Thus, $\langle J, \partial_s \mu_s \rangle^s = \lim_{n \rightarrow \infty} \langle dJ \cdot v^n, \mu \rangle = \langle dJ \cdot v, \mu \rangle$. Choosing a constant $c \geq \sup_{x \in M} \|(dJ)_x\| A/(1 - \lambda)$,

$$(9.1) \quad |(dJ)_x \cdot v_x^n - (dJ)_x \cdot v_x| < c \lambda^n \quad \forall x \in M, n \in \mathbb{Z}^+.$$

Let x be an arbitrary point on M chosen μ -a.e. As usual, we use the shorthand f_n to represent f_{x_n} , the vector field f evaluated at the point x_n . The error in the N -time ergodic average is as follows,

$$(9.2) \quad \left| \frac{1}{N} \sum_{n=0}^{N-1} (dJ)_n \cdot (v_n^n - v_n) \right| \leq \frac{c}{N} \sum_{n=0}^{N-1} \lambda^n := \frac{c_1}{N}.$$

Thus, the error in the stable contribution computation can be bounded as follows.

$$(9.3) \quad \left| \frac{1}{N} \sum_{n=0}^{N-1} (dJ)_n \cdot v_n^n - \langle dJ \cdot v, \mu \rangle \right| \leq \left| \frac{1}{N} \sum_{n=0}^{N-1} (dJ)_n \cdot (v_n^n - v_n) \right| + \left| \frac{1}{N} \sum_{n=0}^{N-1} (dJ)_n \cdot v_n - \langle dJ \cdot v, \mu \rangle \right| \\ \leq \frac{c_1}{N} + \frac{c_2 \sqrt{\log \log N}}{\sqrt{N}}.$$

The bound $c_2 \sqrt{\log \log N} / \sqrt{N}$ appears since $(dJ) \cdot v$ is Hölder continuous, and the law of the iterated logarithm [25][43] applies to the convergence of its ergodic sum. Thus, we conclude that the error in the stable contribution computation converges, with N – the trajectory length or the number of sample points according to μ – similar to a typical Monte Carlo integration up to an iterated logarithmic factor,

$$(9.4) \quad \left| \frac{1}{N} \sum_{n=0}^{N-1} (dJ)_n \cdot v_n^n - \langle dJ \cdot v, \mu_s \rangle \right| \sim \mathcal{O}(\sqrt{\log \log N} / \sqrt{N}).$$

9.2. Convergence of the unstable contribution. We establish the convergence of the unstable contribution with the help of two lemmas. The first shows the convergence of the recursive formula for the logarithmic density gradient, g . The second lemma, Lemma 8.11, proves the convergence of the iterative procedure to differentiate the regularized perturbation field, v , on the unstable manifold. Together, these two results can be used to show that the unstable contribution, with the computation described in the S3 algorithm (section 4.1), converges.

9.2.1. Convergence of logarithmic density gradient.

Lemma 9.2. *Given a bounded scalar field r , there exists a unique, bounded scalar field g that satisfies*

$$(9.5) \quad g \circ \varphi = \frac{g}{\alpha \circ \varphi} + r \circ \varphi,$$

Note that when $r = -\gamma/\alpha$, the logarithmic density gradient function satisfies Eq. 9.5.

Proof. First we show existence. Let $h^0 : M \rightarrow \mathbb{R}$ be an arbitrary bounded scalar function. Consider the sequence of scalar functions $\{h^n\}$ which follow the recurrence relation:

$$(9.6) \quad h^{n+1} \circ \varphi = \frac{h^n}{\alpha \circ \varphi} + r \circ \varphi.$$

We show that this sequence converges uniformly. From the above recurrence relation, at every $x \in M$,

$$(9.7) \quad h_x^{n+1} - h_x^n = \frac{h_{\varphi^{-1}x}^n}{\alpha_x} - \frac{h_{\varphi^{-1}x}^{n-1}}{\alpha_x}.$$

Applying this relation recursively, for all $n \geq 1$,

$$(9.8) \quad |h_x^{n+1} - h_x^n| \leq \frac{1}{\prod_{k=0}^{n-1} \alpha_{\varphi^{-k}x}} |h_{\varphi^{-n}x}^1 - h_{\varphi^{-n}x}^0|.$$

Under the assumption of uniform hyperbolicity, there exist constants $C > 0$ and $\lambda \in (0, 1)$ such that $\prod_{k=0}^{n-1} \alpha_{\varphi^{-k}x} \geq (1/C)\lambda^{-n}$, for all $x \in M$. Thus,

$$(9.9) \quad |h_x^{n+1} - h_x^n| \leq C\lambda^n |h_{\varphi^{-n}x}^1 - h_{\varphi^{-n}x}^0|.$$

Since h^0 is a bounded function, and h^1 is also a bounded function because h^0 and r are bounded, there exists $A > 0$ such that $|h_x^1 - h_x^0| \leq A$, for all $x \in M$. Thus, for all $i > j \geq 0$,

$$(9.10) \quad |h_x^i - h_x^j| \leq \sum_{n=j}^{i-1} |h_x^{n+1} - h_x^n| \leq A C \frac{\lambda^j}{1-\lambda}.$$

Hence $\{h^n\}$ is a uniformly Cauchy sequence and therefore converges uniformly. Let $g := \lim_{n \rightarrow \infty} h^n$. We show that this limit is unique. Let $\{h^n\}$ and $\{\tilde{h}^n\}$ be two different sequences satisfying Eq. 9.6. Additionally, assume that both h^0 and \tilde{h}^0 are bounded functions. Then,

$$(9.11) \quad |h_x^n - \tilde{h}_x^n| \leq \frac{|h_{\varphi^{-1}x}^{n-1} - \tilde{h}_{\varphi^{-1}x}^{n-1}|}{\alpha_{\varphi^{-1}x}},$$

which by iteration, gives,

$$(9.12) \quad |h_x^n - \tilde{h}_x^n| \leq \frac{|h_{\varphi^{-n}x}^0 - \tilde{h}_{\varphi^{-n}x}^0|}{\prod_{k=1}^n \alpha_{\varphi^{-k}x}} \leq C \lambda^n |h_{\varphi^{-n}x}^0 - \tilde{h}_{\varphi^{-n}x}^0|.$$

Thus $|h_x^n - \tilde{h}_x^n| \rightarrow 0$ as $n \rightarrow \infty$ since $|h_{\varphi^{-n}x}^0 - \tilde{h}_{\varphi^{-n}x}^0| < \text{const}$. Since this holds for all $x \in M$, $\lim_{n \rightarrow \infty} h^n = \lim_{n \rightarrow \infty} \tilde{h}^n = g$.

We have shown that the limit g is independent of the initial condition h^0 . Hence, without loss of generality, we may assume that $h_x^0 = 0$ at all $x \in M$, as we do in section 6.2. We remark that, due to the algebraic simplification introduced in section 6.4, the explicit iteration of Eq. 9.6 is subsumed under the combination of Eq. 6.25 and 6.26.

9.2.2. Convergence of the unstable contribution computation. In the S3 algorithm, the computation of the unstable contribution is carried out as an ergodic average. We use the results we have set up so far to show that this ergodic average converges to the true unstable contribution. From our derivation (section 5.4) and the strong decay of correlations assumption (section 6.4), we obtain the following regularized expression for the unstable contribution,

$$(9.13) \quad \langle J, \partial_s \mu_s \rangle^u = - \sum_{k=0}^{\infty} \langle J \circ \varphi^k(a g + b), \mu \rangle.$$

In order to show that our computation of the unstable contribution converges, we first note that, due to exponential decay of correlations between Hölder continuous functions (section 5.4), the above series converges. Further, we show in Lemmas 8.8, 8.11 and 9.2 that the convergence to the true values of a , b and g respectively is exponential in each case, along any μ -typical orbit. Thus, iterating the equations for these quantities for a sufficient run-up time, we may assume that they are, up to machine precision, equal to their true values. The convergence rate of the unstable contribution is thus determined by that of the following N -sample averages, at the first few $k \in \mathbb{Z}^+$,

$$(9.14) \quad \left| \sum_{k=0}^{K-1} \left(\langle J \circ \varphi^k(a g + b), \mu \rangle - \frac{1}{N} \sum_{n=0}^{N-1} J_{n+k}(a_n g_n + b_n) \right) \right| \leq \frac{\sum_{k < K} c_k \sqrt{\log \log N}}{\sqrt{N}}.$$

The almost sure error bound of $\mathcal{O}(\sqrt{\log \log N}/\sqrt{N})$ again appears because of the law of the iterated logarithm, which holds for Hölder continuous functions [25][43]. Given $\epsilon > 0$, there exists a K such that $|\sum_{k > K} \langle J \circ \varphi^k(a g + b), \mu \rangle| < \epsilon/2$, due to the convergence of (9.13). Then, choosing N large enough such that $\sum_{k < K} c_k \sqrt{\log \log N}/\sqrt{N} < \epsilon/2$, we approximate the unstable contribution arbitrarily well, $|\langle J, \partial_s \mu_s \rangle^u - \sum_{k=0}^{K-1} (1/N) \sum_{n=0}^{N-1} J_{n+k}(a_n g_n + b_n)| < \epsilon$. This numerical approximation converges to the unstable contribution as $N \rightarrow \infty$ followed by as $K \rightarrow \infty$. We have already shown that the stable contribution computation has an error convergence rate of $\mathcal{O}(\sqrt{\log \log N}/\sqrt{N})$ (Lemma 9.1). This proves that the sum of stable and unstable contribution converges (discounting the bias due to a finite K) as $\mathcal{O}(\sqrt{\log \log N}/\sqrt{N})$, with the S3 algorithm implemented on an N -length trajectory.

10. Discussion and conclusion. The main contribution of this paper is a new algorithm, called space-split sensitivity (S3), to compute linear response, or the sensitivities of statistics to parameters, in chaotic dynamical systems. The paper presents the derivation of S3 with Ruelle's linear response formula as the starting point. While Ruelle's formula leads to an ill-conditioned direct computation, we derive a decomposition – the S3 decomposition – of the formula that yields a well-conditioned ergodic-averaging computation. The S3 decomposition is achieved by orthogonalizing the conventional tangent solution with respect to the unstable subspaces along a long trajectory. This procedure yields a regularized tangent vector field v and a scalar field a .

The sensitivity to the unstable vector field so achieved – $a g$ – is called the unstable contribution. The stable contribution is the remaining linear response, and can be calculated just as tangent sensitivities are in non-chaotic systems, but using the regularized tangent solutions in place of the conventional tangent solutions. The unstable contribution is integrated by parts on the unstable manifold to yield an expression in which, unlike the original form of Ruelle's formula, the integrand is bounded at all times. Then, exploiting the decay of correlations, this regularized formula can be computed fast as a sum of Monte Carlo integrals. However, the problem is, we obtain two unknown functions – the derivative of a on the unstable manifold, and the density gradient. The density gradient is a fundamental object whose regularity we link, in a different study [64], to the validity of linear response [61][60].

The density gradient is the unstable derivative of the logarithmic conditional density of the SRB measure on the unstable manifold. We take the unstable derivative of Pesin's formula

to obtain a recursive evaluation of the density gradient along a typical trajectory. We show that starting this recursion with an arbitrary scalar field leads to an exponential convergence to the true density gradient. A recursive procedure is also derived for the unstable derivative of a by combining the unstable derivatives of v and q . The evaluation of the latter two unstable derivatives requires solving two second-order tangent equations, which are the most computationally intensive steps of the S3 algorithm.

Overall, the S3 algorithm computes Ruelle's formula as a well-conditioned ergodic average. The efficiency of the S3 algorithm stems from its decomposition of Ruelle's formula and its treatment of the unstable contribution. In Ruelle's formula (Eq. 3.11), the norm of the integrand increases exponentially with n , which leads to the ill-conditioning of the estimation of each term as an ergodic average. However, in the unstable contribution after applying the S3 decomposition (Eq. 5.11), the norm of the integrand does not grow with n and hence, the estimation of the S3 formula as an ergodic average is efficient.

An important direction of future work is to make S3 applicable to systems with higher-dimensional unstable manifolds. Instead of being one-dimensional, as we have assumed throughout this paper, suppose E_x^u is an $m_u \geq 1$ dimensional subspace at each $x \in M$. We anticipate that the S3 algorithm then involves the following changes, which will be pursued in a future work:

1. We must compute, e.g. using Ginelli's algorithm [30], an orthonormal basis for the unstable subspaces along an orbit. This more general procedure reduces to Step 2 of the S3 algorithm (section 4.1), in the case of a 1D unstable manifold. Let $q_{x_n}^i, 1 \leq i \leq m_u, 1 \leq n \leq N$ be the resultant orthogonal tangent vectors that span $E_{x_n}^u, 1 \leq n \leq N$.
2. The regularized tangent equation must now be orthogonalized with respect to the computed unstable subspaces along the trajectory, as opposed to with respect to a single direction. This orthogonalization results in a regularized tangent vector field v and m_u different scalar fields, $a^i, 1 \leq i \leq m_u$, in place of a single scalar field a . The stable contribution may be computed using v just as in the 1D unstable manifold case (Eq. 5.5).
3. The first step in treating the unstable contribution is the integration by parts on the unstable manifold. In the multi-dimensional unstable manifold case, the parameterization Φ^x is now a map from $[0, 1]^{m_u}$ to Ξ_x , such that $\nabla_\xi \Phi^{x_n}(0)$ maps the standard Euclidean basis vector e^i in \mathbb{R}^{m_u} to $q_{x_n}^i$. Using disintegration followed by integration by parts on the m_u -dimensional unstable manifold results in a regularized expression for the unstable contribution, analogous to the 1D case (Eq. 5.9),

$$(10.1) \quad \langle J, \partial_s \mu_s \rangle^u = - \sum_{n=0}^{\infty} \langle J \circ \varphi^n (a \cdot g + \text{div}^u a), \mu \rangle.$$

Here $a : M \rightarrow \mathbb{R}^{m_u}$ and $g : M \rightarrow \mathbb{R}^{m_u}$ are now vector-valued functions on M . The term $\text{div}^u a$ refers to the unstable divergence of the unstable perturbation field $\sum_i a^i q^i$. Now, analogous to the computation of $ag + b$ in the 1D unstable manifold, which we tackled in this paper, we must derive a new computation for the derivative of $a \cdot g + \text{div}^u a$. Such a computation must similarly be recursive so that it can be efficiently carried out using information available along an orbit.

Since we used the unstable derivatives of α , v and q in the computation of $ag + b$ in the 1D unstable manifold case, we expect analogous derivatives are necessary in higher dimensions. In particular, the unstable derivatives – which are m_u -dimensional gradients, i.e., partial derivatives taken with respect to each ξ^i corresponding to q^i – of v and each q^i are needed. The higher dimensional analog of α are the diagonal elements of the R matrix in the QR-based iterative computation in Ginelli’s algorithm; the unstable gradient of the diagonal elements of R are needed. Computing these required derivatives efficiently is the crux of this future direction that will enable the application of S3 to systems with arbitrary dimensional unstable manifolds.

From the outline sketched above, it is amply clear that the S3 algorithm presented here serves as an excellent starting point from which to extend to higher-dimensional unstable manifolds. Moreover, we have proved the existence of the S3 decomposition and the convergence of the algorithm in uniformly hyperbolic systems. The proof of convergence presented in this paper is also readily extensible to the case of higher-dimensional unstable manifolds. Here we have shown that both the stable and unstable contributions to the sensitivity, computed as per the S3 algorithm, have an error convergence that declines as a Monte Carlo computation of an ergodic average. Thus, this work is the first step toward circumventing the poor convergence rate of Ruelle’s formula for linear response.

Acknowledgments. We are greatly indebted to Malo Jézéquel, the anonymous reviewers, Youssef Marzouk and Angxiu Ni for pointing out errors and substantially improving the manuscript.

REFERENCES

- [1] R. V. ABRAMOV AND A. J. MAJDA, *Blended response algorithms for linear fluctuation-dissipation for complex nonlinear dynamical systems*, *Nonlinearity*, 20 (2007), pp. 2793–2821, <https://doi.org/10.1088/0951-7715/20/12/004>, <https://doi.org/10.1088/0951-7715/20/12/004>.
- [2] P. ASHWIN AND A. VON DER HEYDT, *Extreme sensitivity and climate tipping points*, *J Stat Phys*, 179 (2020), pp. 1531–1552, <https://doi.org/10.1007/s10955-019-02425-x>.
- [3] W. BAHSOUN, S. GALATOLO, I. NISOLI, AND X. NIU, *A rigorous computational approach to linear response*, *Nonlinearity*, 31 (2018), pp. 1073–1109, <https://doi.org/10.1088/1361-6544/aa9a88>.
- [4] W. BAHSOUN AND B. SAUSSOL, *Linear response in the intermittent family: Differentiation in a weighted c^0 -norm*, *Discrete & Continuous Dynamical Systems*, 36 (2016), pp. 6657–6668, <https://doi.org/10.3934/dcds.2016089>.
- [5] V. BALADI AND D. SMANIA, *Linear response for smooth deformations of generic nonuniformly hyperbolic unimodal maps*, *Annales scientifiques de l’ENS*, 45 (2012), pp. 861–926.
- [6] V. BALADI AND M. TODD, *Linear response for intermittent maps*, *Commun. Math. Phys.*, 347 (2016), pp. 857–874, <https://doi.org/10.1007/s00220-016-2577-z>.
- [7] P. J. BLONIGAN, *Adjoint sensitivity analysis of chaotic dynamical systems with non-intrusive least squares shadowing*, *Journal of Computational Physics*, 348 (2017), pp. 803–826, <https://doi.org/10.1016/j.jcp.2017.08.002>.
- [8] P. J. BLONIGAN, M. FARAZMAND, AND T. P. SAPSIS, *Are extreme dissipation events predictable in turbulent fluid flows?*, *Phys. Rev. Fluids*, 4 (2019), p. 044606, <https://doi.org/10.1103/PhysRevFluids.4.044606>, <https://link.aps.org/doi/10.1103/PhysRevFluids.4.044606>.
- [9] T. BOMFIM, A. CASTRO, AND P. VARANDAS, *Differentiability of thermodynamical quantities in non-uniformly expanding dynamics*, *Advances in Mathematics*, 292 (2016), pp. 478–528, <https://doi.org/https://doi.org/10.1016/j.aim.2016.01.017>, <https://www.sciencedirect.com/science/article/pii/S000187081600044X>.

- [10] T. BÓDAI, V. LUCARINI, AND F. LUNKEIT, *Can we use linear response theory to assess geoengineering strategies?*, *Chaos: An Interdisciplinary Journal of Nonlinear Science*, 30 (2020), p. 023124, <https://doi.org/10.1063/1.5122255>, <https://doi.org/10.1063/1.5122255>, <https://arxiv.org/abs/https://doi.org/10.1063/1.5122255>.
- [11] M. CENCINI AND F. GINELLI, *Lyapunov analysis: from dynamical systems theory to applications*, *Journal of Physics A: Mathematical and Theoretical*, 46 (2013), p. 250301, <https://doi.org/10.1088/1751-8113/46/25/250301>, <https://doi.org/10.1088/1751-8113/46/25/250301>.
- [12] B. CESSAC, *Linear response in neuronal networks: From neurons dynamics to collective response*, *Chaos*, 29 (2019), p. 103105, <https://doi.org/10.1063/1.5111803>.
- [13] N. CHANDRAMOORTHY, *nishachandramoorthy/s3: Differential clv method*, 1.0.0, (2020), <https://doi.org/10.5281/zenodo.3941678>, <https://doi.org/10.5281/zenodo.3941678>.
- [14] N. CHANDRAMOORTHY, P. FERNANDEZ, C. TALNIKAR, AND Q. WANG, *Feasibility analysis of ensemble sensitivity computation in turbulent flows*, *AIAA Journal*, 57 (2019), pp. 4514–4526, <https://doi.org/10.2514/1.J058127>, <https://doi.org/10.2514/1.J058127>, <https://arxiv.org/abs/https://doi.org/10.2514/1.J058127>.
- [15] N. CHANDRAMOORTHY, L. MAGRI, AND Q. WANG, *Variational optimization and data assimilation in chaotic time-delayed systems with automatic-differentiated shadowing sensitivity*, *arXiv e-prints*, (2020), arXiv:2011.08794, p. arXiv:2011.08794, <https://arxiv.org/abs/2011.08794>.
- [16] N. CHANDRAMOORTHY AND Q. WANG, *Sensitivity computation of statistically stationary quantities in turbulent flows*, in *AIAA Aviation 2019 Forum*, 2019, <https://doi.org/10.2514/6.2019-3426>, <https://arc.aiaa.org/doi/pdf/10.2514/6.2019-3426>, <https://arxiv.org/abs/https://arc.aiaa.org/doi/pdf/10.2514/6.2019-3426>.
- [17] N. CHANDRAMOORTHY AND Q. WANG, *A computable realization of Ruelle’s formula for linear response of statistics in chaotic systems*, *arXiv e-prints*, (2020), arXiv:2002.04117, p. arXiv:2002.04117, <https://arxiv.org/abs/2002.04117>.
- [18] N. CHANDRAMOORTHY AND Q. WANG, *An ergodic averaging method to differentiate covariant Lyapunov vectors*, *Nonlinear Dyn.*, 104 (2021), pp. 4083–4102, <https://doi.org/10.1007/s11071-021-06478-0>.
- [19] N. CHANDRAMOORTHY AND Q. WANG, *On the probability of finding nonphysical solutions through shadowing*, *Journal of Computational Physics*, 440 (2021), p. 110389, <https://doi.org/10.1016/j.jcp.2021.110389>, <https://www.sciencedirect.com/science/article/pii/S0021999121002849>.
- [20] M. CHATER, A. NI, P. BLONIGAN, AND Q. WANG, *Least squares shadowing method for sensitivity analysis of differential equations*, *SIAM J. Numer. Anal.*, 55 (2017), pp. 3030–3046, <https://doi.org/10.1137/15M1039067>.
- [21] M. D. CHEKROUN, J. D. NEELIN, D. KONDRASHOV, J. C. MCWILLIAMS, AND M. GHIL, *Rough parameter dependence in climate models and the role of ruelle-pollicott resonances*, *Proceedings of the National Academy of Sciences*, 111 (2014), pp. 1684–1690, <https://doi.org/10.1073/pnas.1321816111>.
- [22] N. I. CHERNOV, *Limit theorems and markov approximations for chaotic dynamical systems*, *Probability Theory and Related Fields*, 101 (1995), pp. 321–362, <https://doi.org/10.1007/BF01200500>, <https://doi.org/10.1007/BF01200500>.
- [23] V. CLIMENHAGA AND A. KATOK, *Measure theory through dynamical eyes*, 2012, <https://arxiv.org/abs/1208.4550>.
- [24] B. DE LEEUW, S. DUBINKINA, J. FRANK, A. STEYER, X. TU, AND E. V. VLECK, *Projected shadowing-based data assimilation*, *SIAM J. Appl. Dyn. Syst.*, 17 (2018), pp. 2446–2477, <https://doi.org/10.1137/17M1141163>.
- [25] M. DENKER AND W. PHILIPP, *Approximation by brownian motion for gibbs measures and flows under a function*, *Ergodic Theory and Dynamical Systems*, 4 (1984), p. 541–552, <https://doi.org/10.1017/S0143385700002637>.
- [26] D. DOLGOPYAT, *On differentiability of srb states for partially hyperbolic systems*, *Inventiones Mathematicae*, 155 (2004), pp. 389–449, <https://search.proquest.com/docview/881392378?accountid=12492>. Copyright - Springer-Verlag 2004; Last updated - 2012-06-29.
- [27] S. DYATLOV, *Notes on hyperbolic dynamics*, 2018, <https://arxiv.org/abs/1805.11660>.
- [28] G. EYINK, T. HAINE, AND D. LEA, *Ruelle’s linear response formula, ensemble adjoint schemes and lévy flights*, *Nonlinearity*, 17 (2004), p. 1867, <https://doi.org/10.1088/0951-7715/17/5/016>.
- [29] S. GALATOLO AND P. GIULIETTI, *A linear response for dynamical systems with additive noise*, *Nonlin-*

- earity, 32 (2019), pp. 2269–2301, <https://doi.org/10.1088/1361-6544/ab0c2e>.
- [30] F. GINELLI, H. CHATÉ, R. LIVI, AND A. POLITI, *Covariant lyapunov vectors*, Journal of Physics A: Mathematical and Theoretical, 46 (2013), p. 254005, <https://doi.org/10.1088/1751-8113/46/25/254005>.
- [31] S. GOUËZEL, C. LIVERANI, ET AL., *Compact locally maximal hyperbolic sets for smooth maps: fine statistical properties*, Journal of Differential Geometry, 79 (2008), pp. 433–477, <https://doi.org/10.4310/jdg/1213798184>.
- [32] M. HAIRER AND A. J. MAJDA, *A simple framework to justify linear response theory*, Nonlinearity, 23 (2010), pp. 909–922, <https://doi.org/10.1088/0951-7715/23/4/008>, <https://doi.org/10.1088/0951-7715/23/4/008>.
- [33] B. HASSELBLATT AND A. WILKINSON, *Prevalence of non-Lipschitz Anosov foliations*, Ergodic Theory and Dynamical Systems, 19 (1999), pp. 643–656, <https://doi.org/10.1017/S0143385799133868>. Publisher: Cambridge University Press.
- [34] M. JIANG, *Differentiating potential functions of srb measures on hyperbolic attractors*, Ergodic Theory and Dynamical Systems, 32 (2012), pp. 1350–1369, <https://doi.org/10.1017/S0143385711000241>.
- [35] A. KATOK AND B. HASSELBLATT, *Introduction to the modern theory of dynamical systems*, vol. 54, Cambridge university press, 1997, <https://doi.org/10.1017/CBO9780511809187>.
- [36] D. LASAGNA, *Sensitivity analysis of chaotic systems using unstable periodic orbits*, SIAM Journal on Applied Dynamical Systems, 17 (2018), pp. 547–580, <https://doi.org/10.1137/17M114354X>, <https://doi.org/10.1137/17M114354X>, <https://arxiv.org/abs/https://doi.org/10.1137/17M114354X>.
- [37] D. J. LEA, M. R. ALLEN, AND T. W. HAINE, *Sensitivity analysis of the climate of a chaotic system*, Tellus A: Dynamic Meteorology and Oceanography, 52 (2000), pp. 523–532, <https://doi.org/10.1034/j.1600-0870.2000.01137.x>.
- [38] F. LEDRAPPIER AND L.-S. YOUNG, *The metric entropy of diffeomorphisms: Part i: Characterization of measures satisfying pesin’s entropy formula*, Annals of Mathematics, 122 (1985), pp. 509–539, <http://www.jstor.org/stable/1971328>.
- [39] C. LIVERANI, *Central limit theorem for deterministic systems*, in International Conference on Dynamical Systems (Montevideo, 1995), vol. 362, 1996, pp. 56–75.
- [40] V. LUCARINI, *Stochastic perturbations to dynamical systems: A response theory approach*, J Stat Phys, 146 (2012), pp. 774–786, <https://doi.org/10.1007/s10955-012-0422-0>.
- [41] V. LUCARINI, R. BLENDER, C. HERBERT, F. RAGONE, S. PASCALE, AND J. WOUTERS, *Mathematical and physical ideas for climate science*, Rev. Geophys., 52 (2014), pp. 809–859, <https://doi.org/10.1002/2013RG000446>.
- [42] V. LUCARINI AND T. BÓDAI, *Transitions across melancholia states in a climate model: Reconciling the deterministic and stochastic points of view*, Phys. Rev. Lett., 122 (2019), p. 158701, <https://doi.org/10.1103/PhysRevLett.122.158701>, <https://link.aps.org/doi/10.1103/PhysRevLett.122.158701>.
- [43] I. MELBOURNE AND M. NICOL, *A vector-valued almost sure invariance principle for hyperbolic dynamical systems*, The Annals of Probability, 37 (2009), pp. 478 – 505, <https://doi.org/10.1214/08-AOP410>, <https://doi.org/10.1214/08-AOP410>.
- [44] A. NI, *Hyperbolicity, shadowing directions and sensitivity analysis of a turbulent three-dimensional flow*, Journal of Fluid Mechanics, 863 (2019), p. 644–669, <https://doi.org/10.1017/jfm.2018.986>.
- [45] A. NI, *Approximating linear response by non-intrusive shadowing algorithms*, arXiv e-prints, (2020), arXiv:2003.09801, p. arXiv:2003.09801, <https://arxiv.org/abs/2003.09801>.
- [46] A. NI, *Linear response algorithm for differentiating stationary measures of chaos*, arXiv e-prints, (2020), arXiv:2009.00595, p. arXiv:2009.00595, <https://arxiv.org/abs/2009.00595>.
- [47] A. NI AND C. TALNIKAR, *Adjoint sensitivity analysis on chaotic dynamical systems by non-intrusive least squares adjoint shadowing (nilsas)*, Journal of Computational Physics, 395 (2019), pp. 690 – 709, <https://doi.org/https://doi.org/10.1016/j.jcp.2019.06.035>, <http://www.sciencedirect.com/science/article/pii/S0021999119304437>.
- [48] A. NI AND Q. WANG, *Sensitivity analysis on chaotic dynamical systems by non-intrusive least squares shadowing (nilss)*, Journal of Computational Physics, 347 (2017), pp. 56–77, <https://doi.org/10.1016/j.jcp.2017.06.033>.
- [49] Y. B. PESIN, *Characteristic lyapunov exponents and smooth ergodic theory*, Uspekhi Matematicheskikh Nauk, 32 (1977), pp. 55–112.
- [50] C. PUGH, M. SHUB, A. WILKINSON, ET AL., *Hölder foliations*, Duke Mathematical Journal, 86 (1997),

- pp. 517–546.
- [51] C. QUINN, J. SIEBER, AND A. VON DER HEYDT, *Effects of periodic forcing on a paleoclimate delay model*, SIAM J. Appl. Dyn. Syst., 18 (2019), pp. 1060–1077, <https://doi.org/10.1137/18M1203079>.
 - [52] F. RAGONE, V. LUCARINI, AND F. LUNKEIT, *A new framework for climate sensitivity and prediction: a modelling perspective*, Climate Dynamics, 46 (2016), pp. 1459–1471, <https://doi.org/10.1007/s00382-015-2657-3>.
 - [53] D. RUELE, *Differentiation of srb states*, Communications in Mathematical Physics, 187 (1997), pp. 227–241, <https://doi.org/10.1007/s002200050134>.
 - [54] D. RUELE, *Differentiation of srb states: correction and complements*, Communications in mathematical physics, 234 (2003), pp. 185–190, <https://doi.org/10.1007/s00220-002-0779-z>.
 - [55] D. RUELE, *Differentiation of srb states for hyperbolic flows*, Ergodic Theory and Dynamical Systems, 28 (2008), pp. 613–631, <https://doi.org/10.1017/S0143385707000260>.
 - [56] D. RUELE, *A review of linear response theory for general differentiable dynamical systems*, Nonlinearity, 22 (2009), p. 855, <https://doi.org/10.1088/0951-7715/22/4/009>.
 - [57] A. SLIWIAK, N. CHANDRAMOORTHY, AND Q. WANG, *Ergodic sensitivity analysis of one-dimensional chaotic maps*, Theoretical and Applied Mechanics Letters, 10 (2020), pp. 1–10, <https://doi.org/10.1016/j.taml.2020.01.058>.
 - [58] C. TALNIKAR, Q. WANG, AND G. M. LASKOWSKI, *Unsteady adjoint of pressure loss for a fundamental transonic turbine vane*, Journal of Turbomachinery, 139 (2017), p. 031001, <https://doi.org/10.1115/1.4034800>.
 - [59] Q. WANG, *Convergence of the least squares shadowing method for computing derivative of ergodic averages*, SIAM Journal on Numerical Analysis, 52 (2014), pp. 156–170, <https://doi.org/10.1137/130917065>.
 - [60] C. L. WORMELL AND G. A. GOTTWALD, *On the validity of linear response theory in high-dimensional deterministic dynamical systems*, J Stat Phys, 172 (2018), pp. 1479–1498, <https://doi.org/10.1007/s10955-018-2106-x>.
 - [61] C. L. WORMELL AND G. A. GOTTWALD, *Linear response for macroscopic observables in high-dimensional systems*, Chaos: An Interdisciplinary Journal of Nonlinear Science, 29 (2019), p. 113127, <https://doi.org/10.1063/1.5122740>, <https://doi.org/10.1063/1.5122740>, <https://arxiv.org/abs/https://doi.org/10.1063/1.5122740>.
 - [62] L.-S. YOUNG, *Statistical properties of dynamical systems with some hyperbolicity*, Annals of Mathematics, 147 (1998), pp. 585–650, <https://doi.org/10.2307/120960>.
 - [63] L.-S. YOUNG, *What are srb measures, and which dynamical systems have them?*, Journal of Statistical Physics, 108 (2002), pp. 733–754, <https://doi.org/10.1023/A:1019762724717>.
 - [64] A. A. ŚLIWIAK, N. CHANDRAMOORTHY, AND Q. WANG, *Computational assessment of smooth and rough parameter dependence of statistics in chaotic dynamical systems*, Communications in Nonlinear Science and Numerical Simulation, 101 (2021), p. 105906, <https://doi.org/10.1016/j.cnsns.2021.105906>, <https://www.sciencedirect.com/science/article/pii/S1007570421002185>.

Appendix A. Relationship between v and the shadowing direction. Let $\chi = \chi^u + \chi^s$ be the direct sum decomposition of χ into its E^u and E^s components. In our notation, $\chi^s = \mathcal{S}\chi$. In Ni [46], the shadowing vector field v^{sh} is given by the following expression, which has also been derived in [59][20].

$$(A.1) \quad v^{\text{sh}} = \sum_{n=0}^{\infty} d\varphi^n \chi^s + \sum_{n=1}^{\infty} d\varphi^{-n} \chi^u.$$

Note that each series is well-defined since at every $x \in M$, $\|d\varphi_x^n \chi_x^s\| \leq C\lambda^n \|\chi_x^s\|$ and $\|d\varphi_x^{-n} \chi_x^u\| \leq C\lambda^n \|\chi_x^u\|$. Hence, we can apply the operator \mathcal{P} to the two sequences $\sum_{n=0}^N d\varphi^n \chi^s$ and $\sum_{n=1}^N d\varphi^{-n} \chi^u$, and the resulting sequences converge uniformly. Recall that since $\mathcal{P}\mathcal{S} = \mathcal{P}$, $\mathcal{P}(I - \mathcal{S})$ is zero. Thus, applying \mathcal{P} on the above expression makes the second series on the

right hand side vanish. Hence, using the remark following the proof of Lemma 8.6,

$$(A.2) \quad \mathcal{P}v^{\text{sh}} = \sum_{n=0}^{\infty} \mathcal{P} d\varphi^n \chi^s = \sum_{n=0}^{\infty} \mathcal{P} d\varphi^n \mathcal{S}\chi = v.$$